UNIVERSITY OF CALIFORNIA,
IRVINE

Clinical and Molecular Characterization of 2p16.1-p15 Microduplications: A Genotype-Phenotype Analysis

THESIS

submitted in partial satisfaction of the requirements
for the degree of

MASTER OF SCIENCE

in Genetic Counseling

by

Camille Brooke Cooley

Thesis Committee:
Professor Virginia E. Kimonis, MD, MRCP, Chair
Adjunct Professor Pamela L. Flodman, MSc, MS, LCGC
Katherine Hall, MSBT, MS, LCGC

2021

DEDICATION

To

Dr. Vicki Cassman. I feel lucky to have known such an incredible human being. You were a constant source of inspiration and encouragement for me and the reason I wanted to pursue a genetic counseling career. I am grateful for every day of my life that you were a part of.

My parents, Antoinette Dwan and Gene Cooley. I would not be the person I am without your guidance, love, and endless support. Thank you for everything.

TABLE OF CONTENTS

LIST OF FIGURES

LIST OF TABLES

ACKNOWLEDGEMENTS

I would like to express the deepest appreciation to my thesis committee for their guidance, insight, time, and endless support throughout the culmination of this project, in addition to my entire graduate career at UCI. I am so grateful for the approachable mentorship and encouragement you have shown to me and all of my classmates. Thank you from the bottom of my heart.

I would also like to thank all of the treating physicians who took the time out of their busy schedules to complete this survey and provide such thorough and detailed responses. I am so grateful for your effort to confirm pathogenicity classifications prior to submitting the survey or add additional information that may be relevant to the study, even if it wasn't specifically queried. To the physicians who emailed me afterwards to express excitement regarding the study, thank you for the kindness and the encouragement you showed to a complete stranger.

I would also like to acknowledge the DECIPHER database for the invaluable resource they provide. The DECIPHER database assists in the clinical interpretation of rare genetic variants through global data sharing. This has a profound impact on the eventual resolution of variant classifications. Additionally, this resource can assist in the medical management or surveillance of individuals who carry variants that may be so rare that no reports are available in the literature.

This study makes use of data generated by the Database of Chromosomal Imbalance and Phenotype in Humans (DECIPHER) community (Firth, H.V. et al., 2009).

Individuals who carried out the original analysis and collection of the DECIPHER data bear no responsibility for the further analysis or interpretation of the data in this report.

A full list of centres who contributed to the generation of the data is available from https://deciphergenomics.org/about/stats and via email from contact@deciphergenomics.org. Funding for the DECIPHER project was provided by Wellcome.

I would also like to acknowledge the UCSC Genome Browser, which facilitated much of the visualization and analysis of the genomic data in this report.

UCSC Genome Browser: http://genome.ucsc.edu.

ABSTRACT OF THE THESIS

Clinical and Molecular Characterization of 2p16.1-p15 Microduplications: A Genotype-Phenotype Analysis

by

Camille Brooke Cooley

Master of Science in Genetic Counseling

University of California, Irvine, 2021

Dr. Virginia E. Kimonis, Chair

Advances in genetic testing technology, specifically the development of chromosomal microarray analysis, made it possible to accurately identify submicroscopic duplicated or deleted regions across the genome. Microarray testing is now a first-tier diagnostic test for individuals with unexplained intellectual disability, developmental delay, or congenital anomalies, due to the ability to detect chromosomal alterations much smaller than classic cytogenetic techniques such as karyotype. The widespread use of microarray testing has led to the rapid discovery of novel microduplications and microdeletions, including 2p16.1-p15 Microdeletion Syndrome. While both deletions and duplications within this region are rare, enough patients with 2p16.1p15 microdeletions and a characteristic set of phenotypic features have been reported for the condition to be classified as a distinct syndrome. Individuals with 2p16.1-p15 Microdeletion Syndrome share clinical manifestations including moderate to severe intellectual disability, developmental delay, structural brain abnormalities, and a

distinct pattern of dysmorphic craniofacial features. Reports of patients with microduplications within this same region, however, are much more limited and associated clinical manifestations are still being discovered and characterized.

This study surveyed the treating clinicians of patients with 2p16.1-p15 microduplications, in order to investigate whether a similar syndromic association exists for duplications of this region. Detailed clinical and molecular genetic characteristics of 9 patients with duplications either within or including the 2p16.1-p15 chromosomal region were collected and are presented here. The most common clinical characteristics reported included neurodevelopmental abnormalities (89% cases), structural or signaling brain abnormalities (67% cases), cardiovascular abnormalities (67% cases), and dysmorphic facial features involving the ears (78% cases), periorbital region (67% cases), lips, mouth, or oral region (67% cases), and nose (44%). These findings are consistent with the clinical features reported in previously published cases of 2p16.1p15 microduplications, and interestingly, some of the features reported in patients with 2p16.1p15 microdeletions, suggesting that disruption of genes within this region may have syndromic consequences due to haploinsufficiency or triplosensitivity. Additionally, specific abnormalities appeared to segregate with duplications containing more distal or proximal breakpoints, suggesting that triplosensitivity of specific gene(s) located at either end of the region of interest may be responsible for certain features; however, more research is necessary to confirm this hypothesis. The standardized compilation of detailed phenotype data included in this report provides clinicians with additional information on the features associated with this rare condition, that can be used to

better guide medical management, screening, and genetic counseling, ultimately benefiting patients and their families.

1. INTRODUCTION

1.1 The Evolution of Cytogenetic Techniques

Cytogenetic analysis techniques have evolved rapidly since 1959, when researchers first determined that an extra copy of chromosome 21 caused Down Syndrome, a clinically well-known neurodevelopmental disorder associated with intellectual disability and a recognizable pattern of dysmorphic features (Chial, 2008; Ferguson-Smith, 2015; Lejeune et al., 1959; Li & Andersson, 2009; Mefford, 2009). This finding motivated researchers to investigate whether other recognizable conditions were similarly caused by differences in chromosome number (Ferguson-Smith, 2015). Cytogenetic analysis of individuals with a shared set of clinical features led to the characterization of two additional autosomal aneuploidies: Trisomy 13 and Trisomy 18 (Edwards et al., 1960; Ferguson-Smith, 2015; Ledbetter, 2008; Smith et al., 1960). Over the following decades, researchers rapidly developed increasingly advanced analysis techniques. This not only improved our ability to detect subtle chromosome alterations, but also strengthened our understanding of human genetics and the underlying chromosomal basis of disease (Ledbetter, 2008). As cytogenetic methods evolved, so did the clinical application of molecular genetics. These advances allowed previously undetectable genetic alterations to be found and the use of cytogenetic analysis gradually expanded; studies that were predominantly confined to a research laboratory setting in the past could now be routinely used in clinical management. As the diagnostic utility and use of genetic testing increased, new genetic syndromes began to emerge (Ledbetter, 2008).

The invention of staining methods in the 1970's allowed metaphase chromosomes to be accurately distinguished from one another (Ledbetter, 2008; O'Connor, 2008a). Researchers discovered that various dyes interacted with specific compositions of DNA along the length of a chromosome, generating reproducible banding patterns distinct to a particular chromosome pair (Drets & Shaw, 1971; Ferguson-Smith, 2015; O'Connor, 2008a). Chromosome banding methods had a monumental impact on the field of cytogenetics because for the first time, individual pairs of chromosomes could be accurately sorted and visualized based on their underlying structural composition (Case, 2020; Ferguson-Smith, 2015; Ledbetter, 2008). Prior to the development of chromosome staining, researchers struggled to accurately differentiate and group chromosomes, especially chromosomes similar in size or with similar positioning of the centromere (O'Connor, 2008a). Since the unique composition of each chromosome was not visible before staining, chromosomes could only be sorted into 7 groups based on their overall size, centromere position, and the length of the *p* and *q* arms (Kannan & Zilfalil, 2009; O'Connor, 2008; Spinner, 2013). More specific categorization was not possible without additional information regarding the underlying structural landscape of chromosomes.

The ability to accurately distinguish and characterize each chromosome with banding techniques, initiated a new method of chromosome classification that would eventually become an internationally accepted standard (Jorde et al., 2015; O'Connor, 2008a; Spinner, 2013). Chromosome banding pioneered the development of the first karyogram, a schematic representation of the 23 pairs of chromosomes, arranged to visually enhance comparisons of their underlying structural and morphological

characteristics (Case, 2020; Jorde et al., 2015; Spinner, 2013). While previous cytogenetic techniques could identify common autosomal and sex chromosome aneuploidies in addition to large deletions, duplications, and some translocations, chromosome banding enabled the detection of structural alterations as small as 5-10 Mb along any chromosome, depending on the underlying gene density and specificity of the target region (Ledbetter, 2008; Mefford, 2009; Nussbaum et al., 2015). Further adaptations of traditional chromosome banding increased the resolution of this technique, allowing the detection of chromosome aberrations as small as 3-5 Mb (Ledbetter, 2008; Levy & Burnside, 2019; Li & Andersson, 2009). In traditional banding, cultured cells are arrested in metaphase and chromosomes are stained when in their most condensed state (Jorde et al., 2015; Nussbaum et al., 2015). This yields a resolution of approximately 400-550 bands spread over a complete haploid set of chromosomes (Jorde et al., 2015; Nussbaum et al., 2015). Since the smallest detectable alteration is dictated by the number of visible bands along the length of a chromosome, scientists determined that the resolution of a preparation could be increased by staining less-condensed chromosomes with larger regions of exposed DNA (Houck, 2012). By using cells arrested in prophase or early metaphase, the number of visible bands in a haploid set could be increased to at least 850, allowing the detection of much smaller imbalances (Houck, 2012; Jorde et al., 2015; Nussbaum et al., 2015). The development of high-resolution banding in the 1980's first introduced the concept of contiguous gene deletion syndromes, following the discovery that several clinically-recognized conditions could be attributed to previously undetectable chromosome deletions (Kannan & Zilfalil, 2009; Ledbetter, 2008; Mefford, 2009;

Nussbaum et al., 2015). The increased resolution of this method revealed the underlying chromosomal basis of known disorders such as Prader-Willi and Angelman syndromes, in most cases is proximal deletions on either the paternal or maternal copy of chromosome 15 (Kannan & Zilfalil, 2009; Ledbetter, 2008; Mefford, 2009). This method also made it possible to establish the cytogenetic etiology responsible for other clinically recognized conditions, including Wolf-Hirschhorn, Cri-du-Chat, Langer-Giedion, and Smith-Magenis Syndrome, among others (Durmaz et al., 2015; Kannan & Zilfalil, 2009; Ledbetter, 2008; Mefford, 2009; Shaffer et al., 2007).

The next significant achievement occurred in the 1990's with the development of Fluorescence in situ hybridization (FISH), which integrated the fields of cytogenetics and molecular genetics (Cui et al., 2016; Durmaz et al., 2015; Nussbaum et al., 2015). In this technique, a fluorescent molecule is attached to a short, single-stranded sequence of DNA or RNA (Jorde et al., 2015). This sequence, or probe, contains a series of nucleotides complimentary to a specific target sequence or region of interest (Jorde et al., 2015). If the fluorescently labeled probe is added to a sample of denatured chromosomes, it will locate and hybridize to the complimentary target sequence, if present (Jorde et al., 2015; O'Connor, 2008a). The sample is then visualized with a fluorescent microscope, allowing researchers to rapidly determine whether a patient carries a suspected chromosomal deletion or duplication, based on the number of fluorescent signals observed (Jorde et al., 2015). Part of what makes FISH such a powerful diagnostic tool, is due to the diverse ways it can be utilized and adapted in order to interrogate different types of genetic alterations, both structural and molecular (Nguyen et al., 2012; Wolff, 2013). While detecting the presence or absence of a

particular sequence is one of the most straightforward and well-known applications of this technology, FISH can also be used in conjunction with classic banding techniques to determine the relative location of a gene or target sequence along the length of a particular chromosome (Cui et al., 2016; Kannan & Zilfalil, 2009; O' Connor, 2008b; Jorde et al., 2015). The ability to match sequence data to specific chromosomal bands assisted in the early mapping of several genes and the annotation of the human genome several years later (Chial, 2008; Cui et al., 2016; O' Connor, 2008a; O' Conner, 2008b).

FISH studies have several advantages over routine cytogenetic methods, including the ability to analyze a wider range of sample types (Nguyen et al., 2012; O'Conner, 2008a; Wolff, 2013). Unlike classic cytogenetic techniques, FISH analysis is not restricted to samples with actively dividing metaphase cells and can be performed on a variety of tissues, with both mitotic and non-mitotic cell compositions (Bishop, 2010; Nguyen et al., 2012; Wolff, 2013). In addition to the highly condensed metaphase cells used in routine cytogenetic evaluations, FISH is commonly used to analyze non-dividing interphase cells in various types of cytological preparations, formalin-fixed paraffin-embedded tissues, and fresh or frozen tissues, among others (Bishop, 2010; Cui et al., 2016; Nguyen et al., 2012; O'Conner, 2008a; Wolff, 2013). This versatility greatly expanded the scope and utility of genetic testing because it allowed analysis to occur in instances where classic cytogenetic investigations may not be possible (Bishop, 2010; Li & Andersson, 2009; O'Conner, 2008a; Wolff, 2013). The strength of this technique is apparent in the evaluation of certain hematopoietic malignancies and solid tumors (Bishop, 2010; Cui et al, 2016; Kannan & Zilfalil, 2009; O'Conner, 2008a;

Wolff, 2013). The low mitotic index in these cell lines make it notoriously difficult to obtain samples suitable for routine chromosome analysis (Bishop, 2010; Kulkarni et al, 2012; Li & Andersson, 2009; O'Conner, 2008a; Wolff, 2013). Classic cytogenetic analysis of miscarriages and stillbirths is similarly hindered by the amount of viable tissue, which is often insufficient to culture (Jobanputra et al., 2011; UT Health, 2020). Interphase FISH analysis, however, is useful in testing products of conception for common chromosomal abnormalities, because it does not require actively dividing cells (Cui et al, 2016; Jobanputra et al., 2011; UT Health, 2020; Wolff, 2013). Since suboptimal preparations are more likely to miss clinically relevant chromosome alterations, interphase FISH analysis may provide a higher diagnostic yield in these instances (Jobanputra et al., 2011; Wolff, 2013).

The ability to evaluate non-dividing interphase cells has several additional benefits, including faster turnaround times and increased resolution (Bishop, 2010; Cui et al, 2016; Durmaz et al, 2015; Jorde et al, 2015; Li & Andersson, 2009). Interphase FISH analysis eliminates the costly and time-consuming process of cell culture, allowing results to be obtained in as little as 24 hours compared to the several weeks typically required for routine chromosome studies (Bishop, 2010; Cui et al, 2016; Jorde et al, 2015). This difference in turnaround time can have a significant impact in settings such as prenatal genetics, where follow-up reproductive choices are extremely time-sensitive (Cui et al, 2016; Jorde et al, 2015; Li & Andersson, 2009; Wolff, 2013).

Faster turnaround times also have a significant impact in the cancer clinic (Bishop, 2010; Hammer et al., 2016). The genetic abnormalities present in various types of cancer provide valuable diagnostic and prognostic information to clinicians (Cui et al,

2016; Wolff, 2013). Since this information influences treatment approaches, therapy response, and clinical trial eligibility, faster turnaround times can significantly improve medical management and patient care (Cui et al, 2016; Hammer et al., 2016; Wolff, 2013). While FISH analysis does not replace classic cytogenetic methods in most cases, it allows clinicians to have a much earlier understanding of clinically significant alterations than would be possible with routine chromosome studies (Hammer et al., 2016). This can substantially affect patient outcomes by preventing delays in diagnosis and/or the initiation of treatment with appropriate therapies (Bishop, 2010; Hammer et al., 2016; Wolff, 2013). Various studies have demonstrated the importance of early treatment initiation, with a recent study reporting up to a 13% increase in mortality associated with treatment delays of just four weeks (Hanna et al., 2020; Hammer et al., 2016; Parmar & Chan, 2020). While this study focused on the seven common cancer types (bladder, breast, colon, rectal, lung, cervix, head/neck) that make up 44% of all reported cancers globally, FISH analysis can assist in the prevention of treatment delays for some of these cancers, such as bladder and breast cancer (Ansorge, 2019; Hanna et al., 2020; Hammer et al., 2016; Parmar & Chan, 2020). FISH analysis of urinary cells has proved to be helpful in the initial diagnosis of bladder cancer, and in some cases can yield more reliable detection of abnormal cells (Ansorge, 2019). FISH analysis can also detect bladder cancer recurrences up to three to six months earlier (Ansorge, 2019). Additionally, the specific molecular profile of a tumor often dictates the type of chemotherapy that will be most effective for that individual (Cui et al, 2016; Wolff, 2013). FISH analysis is also a crucial diagnostic tool for the evaluation of patients with acute promyelocytic leukemia (APL), due to the urgency of treatment initiation (Cui

et al., 2016; Wolff, 2013). FISH analysis can rapidly distinguish between APL cases with t(15:17) translocations versus t(11:17) translocations, which is crucial to establish prior to administering treatment with all trans retinoic acid (ATRA), since ATRA treatment of APL with t(11:17) translocations may not be effective (Wolff, 2013). Multiple studies have demonstrated that HER2-amplified breast cancer is less responsive to radiation and hormonal therapies but responds well to targeted therapies such as Herceptin (Ansorge, 2011; Cui et al., 2016; Nguyen et al., 2012). The identification of HER2 amplification highlights the utility of rapid FISH analysis; early knowledge of HER2 status can prevent treatment delays and the use of therapies that are known to be less-effective (Ansorge, 2011; Nguyen et al., 2012).

Compared to classic chromosome analysis techniques, both metaphase and interphase FISH have significantly higher targeted resolution than the 3-5 Mb limit provided by high-resolution banding (Bishop, 2010; Nguyen et al., 2012). Metaphase FISH analysis can typically detect alterations that are ~1 Mb and larger (Jorde et al, 2015). FISH analysis of interphase cells, however, can detect imbalances as small as 50-100 kb, since chromosomes in non-mitotic cells are significantly less condensed (Li & Andersson, 2009; O'Conner, 2008a). Since many recurrent microdeletion and microduplication syndromes are caused by imbalances smaller than 2 Mb, these conditions are not routinely detectable with classic banding methods (Wolff, 2013). As a result, FISH is an essential diagnostic method for many contiguous gene syndromes, including Miller-Dieker syndrome which is caused by a 17p deletion of approximately 2 Mb, and Charcot-Marie-Tooth Type 1A, caused by a 1.5 Mb duplication of a different region of 17p (O'Conner, 2008a; Wolff, 2013). FISH is also routinely used to diagnose

the contiguous gene deletion syndrome, velocardiofacial syndrome (VCF) (Wolff, 2013). This condition is caused by recurrent deletions within 22q11.2 that can range from approximately 1.5-3 Mb in size (Wolff, 2013). While high-resolution banding can sometimes detect the larger ~3 Mb deletions, the less frequent 1.5 Mb deletions can be detected by FISH (Wolff, 2013).

Despite the many benefits provided by each new advancement in cytogenetics, each method had intrinsic limitations confining their use to the interrogation of specific types of alterations. High-resolution banding, for example, is not capable of detecting the subtle, yet clinically relevant deletions, duplications, and translocations responsible for many conditions (Wolff, 2013). Additionally, classic banding methods cannot resolve alterations involving exchanges between two chromosomal regions with similar sequence compositions (Di Gregorio et al., 2014; Sinclair, 2002; Wolff, 2013). Rearrangements of similarly staining material will produce a banding pattern indistinguishable from that of the expected banding pattern (Di Gregorio et al., 2014; Uhrig et al., 1999; Wolff, 2013). While differences in testing methodology allowed FISH to avoid many of the restrictions of classic chromosome studies, FISH had a fundamental limitation of its own: this technique could only be used to identify *known* genetic alterations (Bishop, 2010; Li & Andersson, 2009). As a result, FISH became an instrumental tool with two primary applications: to screen for common, recurrent alterations and to confirm or rule out a suspected diagnosis (Bishop, 2010; Mefford, 2009). FISH is widely used to identify frequent somatic alterations in tumor samples, such as recurrent translocations, aneusomies, gene amplifications, and gene fusions (Cui et al, 2016; Nguyen et al, 2012; Wolff, 2013). For individuals showing clinical signs

of a particular condition, FISH is commonly used to genetically confirm the suspected diagnosis (Mefford, 2009). While both classic chromosome analysis and FISH continue to play essential diagnostic roles in clinical genetics, neither technique is capable of screening the entire genome for many of the subtle imbalances responsible for conditions with unexplained intellectual disability or multiple congenital anomalies. The next achievement in cytogenetics, chromosomal microarray analysis, successfully closed this gap in diagnostic capability.

1.2 Microarray Analysis & Genotype-First Characterization

The development of chromosomal microarray analysis (CMA) is arguably one of the most significant achievements in clinical genetics. Microarray analysis is a genome-wide screening tool capable of detecting submicroscopic imbalances with great accuracy and precision. The value of this technology was apparent even in its earliest stages of development. The concept of microarray analysis was first introduced with the development of comparative genomic hybridization (CGH), an early predecessor of the sophisticated array-based methods used today. Since its release, CGH underwent numerous modifications to address limitations in resolution and functionality (Theisen, 2008). The development of CGH marked a period of rapid innovation in genetic testing technology, that was further accelerated by the completion of the Human Genome Project in 2003 (Durmaz et al., 2015; Theisen, 2008). The mapping of the human genome led to a better understanding of genetic disease and the critical regions throughout the genome where dosage imbalances are likely to be detrimental (Chial, 2008; Nguyen et al., 2012). With this knowledge and access to genome-wide

sequencing data, researchers were able to develop increasingly sensitive and automated testing platforms (Bishop, 2010; Durmaz et al., 2015). The availability of thorough sequencing data allowed testing to transition away from methods with demanding sample preparation, to automated array-based techniques (Bishop, 2010; Durmaz et al., 2015; Theisen, 2008). This data also allowed researchers to design tests with increased specificity in regions expected to be biologically significant (Bishop, 2010; Wolff, 2013). The diagnostic yield and scope of CMA techniques increased significantly from early CGH methods to modern methods with combined array-Comparative Genomic Hybridization (aCGH) and Single Nucleotide Polymorphism (SNP) analysis. This led to the discovery of novel, submicroscopic variants in individuals with previously unexplained birth defects or intellectual disability (Theisen, 2008). The ability to identify previously undetectable alterations in multiple affected individuals had a profound impact, not only for researchers and clinicians, but also for individuals and families affected by rare conditions with unknown etiology. As the use of microarray analysis increased, so did the utility of “genotype-first” approaches to clinical characterization. This method of characterization, along with new data sharing platforms, facilitated the delineation of new syndromes.

The invention of microarray analysis introduced a testing platform that included many of the beneficial aspects of previous analysis methods, without the same limitations (Theisen, 2008). For example, despite high resolution and fast turnaround times, FISH is incompatible with non-specific, genome-wide screening applications, since it was designed as a targeted identification method for specific alterations (Bishop, 2010; Nguyen et al., 2012; Wolff, 2013). In contrast, routine chromosome banding is

capable of genome-wide screening, however, the resolution is poor and sample preparation is demanding. Chromosomal microarray analysis successfully incorporated the powerful resolution of FISH with the genome-wide screening capability of classic cytogenetic analysis methods (Smetana et al., 2011). Like FISH, microarray analysis can detect very subtle alterations with great accuracy, due to the high resolution intrinsic to all hybridization-based procedures. Unlike FISH, however, microarray analysis is not restricted to the detection of *known* or *suspected* alterations (Bishop, 2010; Mefford, 2009; Nguyen et al., 2012; Theisen, 2008). This distinction gave CMA genome-wide screening capabilities, with considerably higher resolution than classic banding methods (Theisen, 2008). CMA is also capable of detecting alterations that may be missed by FISH due to resolution or signal intensity, such as interstitial microdeletions smaller than 190 kb or microduplications with less than 250 nm separation between them (Bishop, 2010; O'Conner, 2008a). Lastly, CMA was not governed by the same technical limitations and sample requirements as prior analysis methods; CMA can directly analyze DNA from a sample of interest, rather than metaphase cells or interphase nuclei (Cui et al., 2016; Durmaz et al., 2015; Theisen, 2008; Wolff, 2013). The ability to detect submicroscopic, genome-wide imbalances with minimal sample preparation quickly established CMA as an essential diagnostic tool.

The earliest form of microarray analysis, Comparative Genomic Hybridization (CGH), was developed in 1992 as a way to more efficiently analyze copy number variants in tumor samples (Bishop, 2010; Durmaz et al., 2015; Theisen, 2008; Wolff, 2013). While early CGH and advanced versions of FISH shared many similarities, these techniques differed in their use of metaphase chromosomes (Kulkarni et al., 2012).

Unlike FISH, CGH directly analyzes genomic DNA from a sample of interest; metaphase chromosomes are utilized only as a substrate upon which genomic DNA analysis takes place. This procedural difference allowed researchers to perform genome-wide screens on a diverse range of sample types, without the need to culture cells (Chial, 2008; Kulkarni et al., 2012; Theisen, 2008). In early CGH analysis, isolated genomic DNA from a tumor sample and normal control is denatured and labeled with different-colored fluorescent molecules (i.e., red fluorescent probes are coupled to tumor DNA and green probes to control DNA) (Bishop, 2010; Chial, 2008; Jorde et al., 2015; Wolff, 2013). These samples are then combined and allowed to hybridize to a reference set of metaphase chromosomes (Bishop, 2020; Jorde et al., 2015; Wolff, 2013). Once bound to complimentary sequences throughout the reference chromosomes, tumor DNA emits a red fluorescent signal and control DNA emits a green fluorescent signal (Chial, 2008; Jorde et al., 2015). This generates a pattern of red, green, and yellow fluorescence down the length of each reference chromosome, corresponding to the amount of tumor and control DNA hybridized at each location. Regions of red fluorescence indicate excess binding of tumor DNA, whereas regions of green fluorescence indicate excess binding of control DNA (Bishop, 2010; Chial, 2008; Jorde et al., 2015). When equal amounts of tumor and control DNA bind to a specific location, the individual red and green signals will merge, producing an intermediate yellow fluorescence (Bishop, 2010; Chial, 2008; Durmaz et al., 2015; Theisen, 2008). Under normal circumstances, both samples should hybridize equally to the metaphase chromosomes due to competitive binding. Regions with excess binding of tumor DNA or control DNA, therefore, represent copy number variants in the sample of interest (Chial,

2008; Durmaz et al., 2015). This technique allowed researchers to easily determine the *type* and *location* of imbalances in tumor samples, based on the color emitted by the fluorescent probes (Chial, 2008; Jorde et al., 2015).

While early CGH provided a genome-wide screening tool capable of directly analyzing genomic DNA, further adaptations were necessary due to limitations in resolution (Bishop, 2010). Since early CGH relied on metaphase chromosomes as a binding substrate, the resolution of CGH was equivalent to traditional chromosome analysis methods (Chial, 2008). Like routine banding, early CGH could only detect larger microscopic imbalances of approximately 5-10 Mb (Jorde et al., 2015; Theisen, 2008; Wolff, 2013). In order to improve the utility of CGH, researchers created array-based CGH (aCGH) methods. The process of CGH and aCGH are nearly identical, aside from the binding substrate. In aCGH, the labeled sample and control DNA are competitively hybridized to a microarray slide, rather than reference chromosomes (Chial, 2008; Theisen, 2008; Wolff, 2013). This slide contains an organized set of single-stranded DNA targets spotted into distinct wells, with each well corresponding to specific mapped locations across the genome (Case, 2020; Chial, 2008; Durmaz et al., 2015; Jorde et al., 2015; Theisen, 2008). The single-stranded DNA targets used in aCGH methods can consist of either large bacterial artificial chromosome fragments (BAC), cDNA, or oligonucleotides (Theisen, 2008; Li & Anderson, 2009). In total, a single microarray can house thousands to hundreds of thousands of individual DNA targets. Depending on whether the array is for research or clinical purposes, these DNA targets can be regularly spaced across the entire genome, focused only within particular regions known to be dose-sensitive or known to be associated with microdeletion and

microduplication syndromes, or a combination of the two (Bejjani & Shaffer, 2006; Jorde et al., 2015; Li & Anderson, 2009; Wolff, 2013). Computational analysis compares the fluorescent signals of the sample and control DNA at each target location on the microarray (Bishop, 2010; Wolff, 2013). As in CGH, regions of genomic imbalance are identified by the signal intensity of the red and green probes within each individual well on the array (Bishop, 2010; Chial, 2008; Theisen, 2008). While the resolution of aCGH depends on the specific array design, this method can typically detect deletions and duplications as small as 50-100 kb (Jorde et al., 2015). The actual resolution may be higher or lower, however, depending on the total number of DNA targets included in the array, the size of each target, and the genomic distance between targets (Bejjani & Shaffer, 2006; Bishop, 2010; Theisen, 2008; Wolff, 2013).

Traditional aCGH arrays were further adapted to include single nucleotide polymorphism (SNP) targets. SNP arrays contain sequence targets for both possible alleles at each single nucleotide polymorphism loci that is included in the array (Nussbaum et al., 2015). In SNP microarrays, a fluorescently labeled sample of interest is hybridized to the SNP targets immobilized on an array. In contrast to CGH and aCGH, a labeled control is not hybridized to the array along with the sample of interest (Nussbaum et al., 2015). Instead, the signal intensity of the sample of interest is individually measured at each SNP target on the array (Kulkarni et al., 2012; Nussbaum et al., 2015). The fluorescent signal intensity at each SNP is then compared to a normalized standard (Jorde et al., 2015; Kulkarni et al., 2012; Nussbaum et al., 2015). Since each SNP loci included in the array has two separate sequence options, one for each possible allele, this analysis can provide beneficial haplotype information (Jorde et

al., 2015; Nussbaum et al., 2015). Depending on the signal intensity for the two options at each SNP loci on the array, this method can detect uniparental disomy and stretches of homozygosity in addition to deletions and duplications of chromosomal regions (Jorde et al., 2015; Kulkarni et al., 2012). The resolution of SNP-based arrays is higher than aCGH and can detect chromosomal imbalances smaller than 20 kb (Jorde et al., 2015; Kulkarni et al., 2012). Currently, most microarrays are designed to include both copy number variant DNA targets and SNP DNA targets, since the additional information provided by SNP loci increases the potential diagnostic yield of clinically relevant abnormalities in certain patient populations (Kulkarni et al., 2012).

Microarray platforms with CNV and SNP targets, also referred to as Cytogenomic Microarrays (CMA), are an essential diagnostic tool in the evaluation of individuals with unexplained intellectual disability (ID), developmental delay (DD), or multiple congenital anomalies (MCA) (Jorde et al., 2015; Miller et al., 2010; Miller, 2021). While CMA is not able to detect balanced alterations or low levels of mosaicism, experts determined that this was not a significant limitation for the purpose of identifying biologically relevant alterations in patients with idiopathic ID, DD, and MCA (Miller et al., 2010). In this patient population, balanced rearrangements are not a common finding, even with traditional karyotype analysis (Miller et al., 2010). Additionally, researchers discovered that *truly* balanced alterations are common in the general population and unlikely to be causative of the phenotype in this particular group of individuals, even if detected (Miller et al., 2010). Moreover, numerous studies found that many of the alterations identified as balanced with traditional karyotype analysis were actually unbalanced at higher resolutions (Miller et al., 2010). In many of these instances, CMA can detect the

imbalance that was missed or misinterpreted by traditional karyotype analysis (Miller et al., 2010). Researchers also determined that low level mosaicism was a rare finding in this group of patients and unlikely to be responsible for the cognitive and phenotypic manifestations of these conditions (Miller et al., 2010).

As more individuals with idiopathic ID, DD, and MCA underwent CMA testing, researchers began to investigate differences in diagnostic yield between CMA and traditional karyotype analysis. While traditional karyotype analysis was previously considered the “gold standard” diagnostic test, studies found that for this particular group of patients, CMA provided a higher diagnostic yield (Jang et al., 2019; Miller et al., 2010). In these studies, CMA detected submicroscopic pathogenic variants in 10-20% of patients with ID, DD, or MCA who had normal karyotype results (Jang et al., 2019; Miller et al., 2010). In 2010, CMA became the recommended first-tier diagnostic testing option for individuals with unexplained ID, DD, and MCA based on these findings (Jang et al., 2019; Miller et al., 2010). While traditional karyotype analysis is still considered the recommended first-line test in many settings, CMA proved advantageous for patients with non-specific dysmorphic features and idiopathic intellectual disability that did not fit a particular known condition (Miller et al., 2010; Jorde et al., 2015; Shaffer et al., 2007).

After CMA became the recommended first-tier diagnostic test in patients with ID, DD, and MCA, the use of CMA increased. As more individuals underwent testing, researchers increasingly discovered novel microdeletions and microduplications (Mefford, 2009). However, since these submicroscopic imbalances were previously undetectable, many of the identified alterations were initially classified as variants of

uncertain significance (VUS) (Miller et al., 2010; Mefford, 2009). Determining the pathogenicity of these variants was further complicated by the discovery that many healthy individuals also carried copy number variants (Bejjani & Shaffer, 2006; Ledbetter, 2008; Mefford, 2009). While this led to logistical and counseling challenges for labs and providers, it also presented an opportunity to utilize genotype-first methods of clinical characterization (Miller et al., 2010). In an effort to resolve the biological significance of these previously unreported variants, global data sharing platforms were also established (Miller et al., 2010).

Before the development of high-resolution genome-wide screening, many conditions were characterized using a “phenotype-first” approach, in which individuals were identified and grouped together based on a shared pattern of physical characteristics before a genetic (or non-genetic) etiology was established (Miller et al., 2010; Shaffer et al., 2007). However, in order for a condition to be characterized using a phenotype-first approach, the disorder must be relatively common, and the features must be distinct, either on their own or when consistently found together in a recognizable pattern (Jorde et al., 2015; Li & Anderson, 2009). Prior to the advent of CMA, most individuals with submicroscopic chromosomal alterations would have remained undiagnosed due to the non-specific features associated with these conditions (Mefford, 2009). However, in the four years following the introduction of CMA analysis, researchers discovered and characterized more than twice the number of genetic syndromes than they had in the previous 20 years (Mefford, 2009). The combination of genotype-first characterization methods and global data sharing enabled

the discovery and characterization of novel syndromes, including the 2p16.1-p15 Microdeletion Syndrome.

1.3 2p16.1-p15 Microdeletion Syndrome

2p16.1-p15 Microdeletion Syndrome is a rare contiguous gene deletion syndrome that was first described in 2007. This disorder is most commonly caused by microdeletions within a 2.5 Mb region of the 2p16.1p15 chromosomal bands, however deletions of various sizes within 2p16.1-p15 have been reported (Bagheri et al., 2016; Shimojima et al., 2015). While the location, size, and gene content can vary among affected individuals, patients with this condition share a core phenotypic presentation, including neurodevelopmental abnormalities, multiple congenital anomalies, and a distinct pattern of dysmorphic craniofacial features (Bagheri et al., 2016; Fannemel et al., 2014; Kniffin, 2016; Rajcan-Separovic et al., 2007; Shimojima et al., 2015; Wohlleber et al., 2011). Neurodevelopmental abnormalities include moderate to severe intellectual disability, global developmental delay, autism spectrum disorder (ASD) or autistic traits, and attention deficit hyperactivity disorder (ADHD) (Bagheri et al., 2016; Félix et al., 2010; Kniffin, 2016). Patients with 2p16.1-p15 microdeletions share a characteristic set of dysmorphic craniofacial features, including microcephaly, receding forehead, bitemporal narrowing, low set ears, hypertelorism, short palpebral fissures, strabismus, ptosis, broad and high nasal bridge, prominent nasal tip, smooth philtrum, and retrognathia (Félix et al., 2010). Other congenital anomalies associated with 2p16.1-p15 Microdeletion Syndrome include urogenital abnormalities such as hydronephrosis, cryptorchidism, and hypoplastic external genitalia, and structural brain

malformations including enlarged ventricles, cortical dysplasia, pachygyria, and hypoplasia of the corpus collosum, cerebellum and pons (Kniffin, 2016; Shimojima et al., 2015). Skeletal abnormalities involving the extremities, such as bilateral camptodactyly, bilateral clinodactyly, and metatarsus adductus are also commonly reported (Fannemel et al., 2014).

The first 2p16.1-p15 microdeletion was reported by Rajcan-Separovic et al. (2007) in two unrelated individuals with overlapping deletions and similar clinical presentations. Both patients were non-verbal at eight and five years of age. Shared clinical characteristics included global developmental delay, moderate intellectual disability, structural brain abnormalities, mild visual impairment secondary to optic nerve hypoplasia, progressive microcephaly, and a similar pattern of dysmorphic facial features (Rajcan-Separovic et al., 2007). The following genes were reported in the overlapping deleted region in both patients: *VRK2, PAPOLG, BCL11A, KIAA1841 PEX13,* and *FANCL* (Rajcan-Separovic et al., 2007).

The first patient is a female evaluated at 8 years of age. During her mother's pregnancy, intrauterine growth restriction (IUGR), polyhydramnios, left hydronephrosis, and uteropelvic obstruction were reported (Rajcan-Separovic et al., 2007). Her measurements after birth were within normal limits; however, she was later diagnosed with progressive microcephaly, transient postnatal growth restriction, and failure to thrive (Rajcan-Separovic et al., 2007). A brain MRI revealed optic nerve hypoplasia, bilateral perisylvian cortical dysplasia, and perisylvian migration disorder, which was associated with pseudobulbar palsy, dysarthria, dysphagia, facial diplegia and drooling (Rajcan-Separovic et al., 2007). Hearing evaluations were normal; however, mild visual

impairment was reported secondary to optic nerve hypoplasia (Rajcan-Separovic et al., 2007). She had neurodevelopmental abnormalities including severe global developmental delay, moderate intellectual disability, attention deficit hyperactivity disorder (ADHD), and autism spectrum disorder (ASD) (Rajcan-Separovic et al., 2007). Spasticity of the lower extremities and severe speech and language delays were reported; at eight years of age, the patient was non-verbal (Rajcan-Separovic et al., 2007). The patient also had multiple congenital anomalies and facial dysmorphism. Craniofacial features included brachycephaly, bitemporal narrowing, flat occiput, broad and high nasal bridge, prominent nasal tip, wide inner canthal distance, telecanthus, short palpebral fissures, strabismus, ptosis, straight eyelashes, smooth philtrum and an everted lower lip (Rajcan-Separovic et al., 2007). Other congenital abnormalities included increased internipple distance, a unilateral non-functioning multicystic kidney, bilateral camptodactyly of the 3^{rd}-5^{th} fingers and metatarsus adductus of the feet (Rajcan-Separovic et al., 2007). Array-CGH analysis revealed a *de novo* 4.5 Mb microdeletion within the 2p16.1-p15 chromosomal region and a paternally inherited 1.2 Mb microdeletion within the Xp22.31 chromosomal band, which includes the steroid sulphatase (STS) gene associated with X-linked ichthyosis (Rajcan-Separovic et al., 2007). The patient's father is affected with X-linked ichthyosis due to steroid sulfatase deficiency; however, he was described as developmentally normal with no reported phenotypic manifestations other than the dermatologic findings associated with X-linked ichthyosis. The authors suspect the proband's phenotype to be caused by the deletion within 2p16.1-p15 rather than the Xp22.31 deletion, for the following reasons: the Xp22.31 microdeletion was inherited from an otherwise unaffected father with none of

the phenotypic manifestations reported in the patient; X-linked ichthyosis is an autosomal recessive nonsyndromic disorder that almost exclusively effects males; cognitive and developmental abnormalities is a rare manifestation, even in affected males; the patient was found to have random X-inactivation (Hand, 2021; Rajcan-Separovic et al., 2007).

The second patient is a male evaluated at 6 years of age. As a neonate, microcephaly, postnatal growth restriction, and feeding difficulty were reported (Rajcan-Separovic et al., 2007). A brain MRI revealed abnormalities, including optic nerve hypoplasia, enlarged 4th ventricle, mild hypoplasia of the inferior cerebellar vermis, small anterior pituitary and pons, and a thick cortex with subcortical hyperintensity due to suspected dysmyelination or cortical dysplasia (Rajcan-Separovic et al., 2007). An EEG detected signaling abnormalities, including disorganized background activity with spike waves in the mid/left frontal/occipital regions (Rajcan-Separovic et al., 2007). He was diagnosed with global developmental delay and moderate intellectual disability (Rajcan-Separovic et al., 2007). He had severe delays in speech and language acquisition and was non-verbal at 5 years of age (Rajcan-Separovic et al., 2007). Autistic features, attention deficits, and spasticity of the lower extremities were also noted (Rajcan-Separovic et al., 2007). Dysmorphic craniofacial features included brachycephaly, bitemporal narrowing, flat occiput, prominent metopic suture, broad and high nasal bridge, prominent nasal tip, wide inner canthal distance, telecanthus, short palpebral fissures, strabismus, ptosis, straight eyelashes and long eyebrows, large ears, smooth philtrum and an everted lower lip (Rajcan-Separovic et al., 2007). He had abnormalities of the extremities including bilateral camptodactyly of the 5th fingers, 2nd-

3rd toe syndactyly, and metatarsus adductus of the feet (Rajcan-Separovic et al., 2007). Other reported characteristics include genitourinary abnormalities including micropenis, small testes, left hydronephrosis, hypothalamic hypogonadism, bilateral sensorineural hearing loss, and mild visual impairment secondary to hyperopia and optic nerve hypoplasia (Rajcan-Separovic et al., 2007). Array-CGH analysis revealed a *de novo* 5.7 Mb microdeletion within the 2p16.1-p15 chromosomal region (Rajcan-Separovic et al., 2007).

Since this initial report by Rajcan-Separovic et al. (2007), additional patients with similar clinical presentations and 2p16.1-p15 deletions of various sizes have been reported in the literature. Bagheri et al. (2016) investigated the smallest region of overlap in published cases of 2p16.1-p15 microdeletions, and found that the *XPO1, USP34, BCL11A, and REL* genes were the most commonly deleted genes (Bagheri et al., 2016). These four genes were presented as potential candidate genes responsible for the phenotypic and neurodevelopmental abnormalities in affected individuals, since they were encompassed by the deletions in over 60% of published cases and have strong evidence of dosage sensitivity (Bagheri et al., 2016). As more patients with 2p16.1-p15 microdeletions were reported, the critical regions and genes responsible for specific abnormalities were further elucidated. In research by Jorgez et al. (2014), six patients with genitourinary defects and overlapping 2p15 microdeletions were reported. Genes within this region (and the *OTX1* gene in particular) were presented as potential candidate genes for the urogenital abnormalities associated with 2p16.1-p15 Microdeletion Syndrome based on these findings and the presence of genitourinary defects in eight other published cases encompassing the same deleted segment

(Jorgez et al., 2014). Research by Shimojima et al. (2015) further examined the relationship between the genomic and clinical characteristics associated with 2p16.1-p15 microdeletions. Upon thorough review of published reports, authors identified a stark difference in the features reported in patients with more distal deletions compared to those with more proximal deletions within the 2p16.1-p15 chromosomal region (Shimojima et al., 2015). Patients with proximal deletions involving the border between the 2p15 and 2p14 chromosomal bands did not present with the pattern of dysmorphic facial features typical in patients with 2p16.1-p15 Microdeletion Syndrome as well as milder intellectual disability (Shimojima et al., 2015; Wohlleber et al., 2011). Patients with more distal deletions encompassing the border between 2p16.1 and 2p15, on the other hand, displayed the characteristic abnormalities associated with 2p16.1-p15 Microdeletion Syndrome (Shimojima et al., 2015).

1.4 2p16.1-p15 Microduplications

While both deletions and duplications within the 2p16.1-p15 chromosomal region are infrequent findings, the latter is much more rare. To date, duplications of this region have only been described in the literature five times. Three additional case reports describe duplications that include all or part of the 2p16.1-p15 chromosomal region but extend beyond the location of interest. These include one report of 2p16.3-p16.1 duplications associated with perisylvian polymicrogyria, one report of a 2p14-p16 duplication associated with dysmorphic facial features and abnormal muscle development of the diaphragm, and one report of a 2p16.1-p13.2 duplication associated

with dysmorphic facial features and hypercalcemia (Amrom et al., 2019; Guilherme et al., 2009; Lodefalk et al., 2015).

The first 2p16.1-p15 microduplication was reported by Mimouni-Bloch et al. (2015) in a male proband with developmental delay, mild intellectual disability, behavioral abnormalities, moderate bilateral hearing loss, and dysmorphic craniofacial features. The child was born at 38 weeks gestation with a birth weight and head circumference in the 3rd and 10th percentiles, respectively (Mimouni-Bloch et al., 2015). The proband failed an otoacoustic emissions test, with the authors reporting moderate bilateral hearing loss mediated by serous otitis media (Mimouni-Bloch et al., 2015). The patient demonstrated delays in both speech and motor development. Mild intellectual disability was also reported, along with challenges in sensory processing (Mimouni-Bloch et al., 2015). The patient also exhibited attention deficit and oppositional behavior; however, autistic behavior was denied (Mimouni-Bloch et al., 2015). Other clinical characteristics included generalized hypotonia, motor dyspraxia, and iron deficiency anemia (Mimouni-Bloch et al., 2015). Mild dysmorphic craniofacial features included puffy eyelids, broad philtrum, and unilateral ear sinus (Mimouni-Bloch et al., 2015). At a later evaluation, the proband's head circumference was within the 75th percentile for his age group (Mimouni-Bloch et al., 2015). Microarray analysis revealed a 1,665 kb *de novo* microduplication within the 2p16.1-p15 chromosomal region, encompassing the following 10 genes: *BCL11A*, *PAPOLG*, *REL*, *PUS10*, *PEX13*, *KIAA1841*, *C2orf74*, *ASHA*, *USP34*, and *XPO1* (Mimouni-Bloch et al., 2015). The following duplication coordinates were reported using the GRCh37/hg19 assembly: 60,150,427-61,816,209 (Mimouni-Bloch et al., 2015).

Pavone et al. (2019) reported a 2p16.1-p15 microduplication in a 12-year-old boy with moderate global developmental delay, seizures, behavioral concerns, congenital anomalies, and dysmorphic craniofacial features. The patient was born at 36 weeks gestation. He was transferred to an incubator and required artificial ventilation for one week after birth due to cyanosis and respiratory distress (Pavone et al., 2019). The proband experienced feeding difficulty, poor growth, and frequent respiratory infections (Pavone et al., 2019). Global developmental delay was reported; the patient walked at five years of age and spoke at 20 months (Pavone et al., 2019). An echocardiogram identified a mild patent arterial duct with left to right shunting (Pavone et al., 2019). At 12 years of age, the proband began experiencing weekly secondarily generalized epileptic seizures that were successfully reduced after treatment with levetiracetam (Pavone et al., 2019). His measurements at this age revealed a weight above the 97th percentile, height in the 90th percentile, and head circumference in the 50th percentile (Pavone et al., 2019). Reported craniofacial features included dolichocephaly, a short, receding forehead, puffy eyelids, protrusion of the mandible, teeth, and lips, puffy cheeks, short nose, broad philtrum, small mouth, and retrognathia (Pavone et al., 2019). The proband's hands were described as short and puffy, with bilateral 5th finger clinodactyly, "finger-like" thumbs, and dysplastic nails (Pavone et al., 2019). The patient also had bilateral syndactyly of the 2nd-3rd toes and cupped distal phalanges (Pavone et al., 2019). The patient was diagnosed with moderate intellectual disability, Tourette syndrome, obsessive-compulsive disorder, and behavioral concerns (Pavone et al., 2019). Dorsal-lumbar scoliosis and hypotonia were also reported (Pavone et al., 2019). An MRI of the brain revealed abnormalities, including widened liquoral spaces

surrounding the cerebral trunk and mild hyperintensity of the bilateral posterior periventricular areas (Pavone et al., 2019). Microarray analysis revealed a *de novo* microduplication within the 2p16.1-p15 chromosomal region, with the following coordinates using the GRCh37/hg19 assembly: 60,294,104-62,030,285 (Pavone et al., 2019). The microduplication was 1.73 Mb in size and encompassed the following 10 genes: *BCL11A*, *PAPOLG*, *REL*, *PUS10*, *PEX13*, *KIAA1841*, *C2orf74*, *ASHA*, *USP34*, and *XPO1* (Pavone et al., 2019).

Chen et al. (2018) described a maternally inherited 2p16.1-p15 microduplication in a female fetus associated with familial intellectual disability. Amniocentesis was performed at 22 weeks gestation due to a family history of intellectual disability in the mother of the pregnancy and both of her sisters; the mother of the pregnancy and one of her sisters had moderate intellectual disability while the eldest sister was diagnosed with mild intellectual disability (Chen et al., 2018). Karyotype and microarray analysis was performed on cultured amniocytes of the fetus and peripheral blood samples of the two sisters diagnosed with moderate intellectual disability (Chen et al., 2018). The authors denied the presence of any behavioral concerns in all three siblings. Karyotype analysis of the fetus and two women revealed a normal 46, XX karyotype (Chen et al., 2018). Microarray analysis revealed that all three individuals were carriers of a 3.24 Mb microduplication within the 2p16.1-p15 chromosomal bands, with the following coordinates using the GRCh37/hg19 assembly: 58,288,588-61,532,538 (Chen et al., 2018). The microduplication encompasses protein coding genes including *VRK2, FANCL, BCL11A, PAPOLG, REL, PUS10, PEX13* and *USP34.* The infant was born full term and no congenital anomalies or dysmorphic features were noted (Chen et al.,

2018). The patient did not show any signs of psychomotor developmental delay at a follow-up evaluation at 8 months of age (Chen et al., 2018). At this age, her head circumference was in the 75th-85th percentile, her weight was in the 5th-15th percentile, and her length was in the 5th-15th percentile (Chen et al., 2018). No additional information on later development was available.

Lovrecic et al. (2018) described four additional patients with 2p16.1-p15 microduplications, two of which are reported in the DECIPHER database. The first patient is a male infant born full term with a birth weight and birth length in the 25th-50th percentile for gestational age and a head circumference in the 97th percentile (Lovrecic et al., 2018). Feeding difficulty and mild jaundice were reported in the neonatal period (Lovrecic et al., 2018). The patient had both psychomotor delays and speech delays; he walked at 21 months of age and was not yet able to speak in complete sentences at 4 years of age (Lovrecic et al., 2018). Mild dysmorphic craniofacial features included a receding forehead, broad/high nasal bridge, sparse eyebrows, epicanthal folds, straight eyelashes, and a pronounced philtrum (Lovrecic et al., 2018). Abnormalities of the hands and feet included bilateral 5th finger clinodactyly and 2nd-3rd toe syndactyly (Lovrecic et al., 2018). Microarray analysis identified a *de novo* 2.00 Mb microduplication within the 2p16.1-p15 chromosomal bands, with the following coordinates using the GRCh37/hg19 assembly: 60,113,626-62,111,114 (Lovrecic et al., 2018).

The second patient was a male infant born at 37 weeks gestation, with a birth weight and birth length in the 10th-25th percentile for gestational age and a head circumference in the 75th-90th percentile (Lovrecic et al., 2018). He was diagnosed with

gastroesophageal reflux within the first months of life; however, no structural abnormalities were identified by abdominal ultrasound. He had mild hypertonia and mild motor delays. Cardiac abnormalities were also noted, including two atrial septal defects and a mild dilation of the right ventricle (Lovrecic et al., 2018). At a follow-up evaluation at 4 years of age, he had a height within the 17th percentile, weight within the 46th percentile, and a head circumference greater than the 97th percentile for his age group, consistent with macrocephaly. Microarray analysis identified a *de novo* 2.06 Mb microduplication within the 2p16.1-p15 chromosomal bands, with the following coordinates using the GRCh37/hg19 assembly: 60,308,869-62,368,583 (Lovrecic et al., 2018).

The third patient described by Lovrecic et al. (2018) is from the DECIPHER database. The male infant was born at 36 weeks gestation, with a birth weight, length, and head circumference in the 50th, 90th, and 97th percentiles, respectively. He had speech delay and learning difficulties. Microarray analysis identified a maternally inherited microduplication within the 2p16.1-p15 chromosomal region, with the following coordinates using the GRCh37/hg19 assembly: 60,236,241-61,848,845. The patient's mother harboring the same microduplication had learning difficulties, epilepsy, and obesity (Lovrecic et al., 2018).

The fourth patient reported by Lovrecic et al. (2018) is also reported in the DECIPHER database. The male proband was born full term; and as a neonate had hypotonia and feeding difficulty. He had mild motor delay and speech delay and was later diagnosed with moderate intellectual disability. Recurrent infections and thrombocytopenia were reported. He also has macrocephaly, small ears, and small

hands. At a follow-up evaluation at 33 years of age, he had a height and weight in the 95th percentile and a head circumference greater than the 97th percentile. Microarray analysis identified a *de novo* 2.09 Mb microduplication within the 2p16.1-p15 chromosomal bands, with the following coordinates using the GRCh37/hg19 assembly: 59,938,734-62,025,519. The smallest region shared between all four cases encompassed the following nine genes: *BCL11A*, *PAPOLG*, *REL*, *PUS10*, *PEX13*, *KIAA1841*, *C2orf74*, *ASHA*, and *USP34* (Lovrecic et al., 2018).

The fifth case report available in the literature on 2p16.1-p15 microduplications was described in research by Chen et al. (2021). The authors report a maternally inherited (mother unaffected) microduplication within the 2p15 chromosomal region in a female fetus with pulmonary artery stenosis, single umbilical artery, and unilateral postaxial polydactyly (Chen et al., 2021). Karyotype and microarray analysis was performed on cultured amniocytes of the fetus identified a 1.391 Mb microduplication within the 2p15 chromosomal band and a normal 46, XX karyotype. Microarray analysis of both parents revealed that the mother was also a carrier of the same duplication. The female infant was born full term and no physical or psychomotor developmental abnormalities were reported at a follow-up evaluation at one year of age. The following coordinates of the duplication were reported using the GRCh37/hg19 assembly: 61,495,220-62,885,679 . The duplicated region encompasses the following seven OMIM genes: *USP34, XPO1, FAM161A, CCT4, COMMD1, B3GNT2, and TMEM17* (Chen et al., 2021).

Amrom et al. (2019)described three unrelated patients with bilateral perisylvian polymicrogyria, dysmorphic facial features, and different yet overlapping *de novo*

interstitial duplications within chromosome 2p. All three patients carried larger duplications that extended beyond the 2p16.1-p15 chromosomal region; however, the locus associated with perisylvian polymicrogyria was narrowed down to a much smaller region spanning the 2p16.3-p16.1 chromosomal bands. The first patient carried a 2p16.3-p13.3 duplication, the second patient carried a 2p23.1-p16.1 duplication, and the third patient carried a 2p24.1-p13.1 duplication. In all three patients, intrauterine growth restriction (IUGR), shared facial characteristics, and brain abnormalities were reported.

The first patient was a male infant born at 40 weeks gestation with a birth weight, length, and occipitofrontal head circumference in the 4th, 8th, and 92nd percentiles, respectively (Amrom et al., 2019). As a neonate, global hypotonia, pyloric stenosis, dyspraxia, and feeding difficulties were noted. An echocardiogram identified mild pulmonary artery stenosis. Brain MRI revealed bilateral perisylvian polymicrogyria that was most prominent at the fronto-basal and right parieto-occipital regions. Evidence of gliosis anterior to the right lateral ventricle was noted as well as brain changes near the right caudate nucleus consistent with prior hemorrhages. The patient also experienced chronic bronchitis and otitis media, leading to unilateral hearing loss. Short stature with delayed bone age was noted, and treatment with growth hormone was initiated. Genitourinary abnormalities included unilateral cryptorchidism. The patient had global developmental delay consisting of moderate motor delays and severe speech and language delays (Amrom et al., 2019). He was later diagnosed with moderate intellectual disability and ADHD (Amrom et al., 2019). Dysmorphic craniofacial features were reported, including macrocephaly, dolichocephaly, frontal bossing, hypertelorism,

broad nasal bridge, thick eyebrows, strabismus, thick upper lip, and low-set and posteriorly rotated ears (Amrom et al., 2019).

The second patient was a female born at 40 weeks gestation with a birth weight, length, and occipitofrontal head circumference in the 12th, 17th, and 39th percentiles, respectively. She experienced postnatal growth delay and global developmental delay, with an unsteady gait and limited speech. Moderate intellectual disability and behavioral concerns such as aggression, temper tantrums, and mood swings were reported. She had dysmorphic facial features that included hypertelorism, strabismus, broad nasal bridge, and low-set ears . The proband was also reported to have mild neck webbing, bilateral elbow contractures, and seizures that began at 15 years of age . No cardiac or genitourinary abnormalities were identified. MRI of the brain revealed bilateral symmetric perisylvian polymicrogyria that was diffuse but most prominent in the posterior frontal, perisylvian and parietal brain regions (Amrom et al., 2019).

The third patient is a male born at 35 weeks and three days gestation with a birth weight, length, and occipitofrontal head circumference in the 1st, 0, and 57th percentiles, respectively. Severe feeding difficulty was noted in the first few weeks of life. The patient was first evaluated two weeks after birth with no follow-up evaluation, so information regarding potential developmental delays or intellectual disability was not reportable. The patient was noted to have dysmorphic craniofacial features, including rounded head contour, prominent occiput, hypertelorism, upturned nares, small jaw, and bilateral, low-set, posteriorly rotated ears. Genitourinary abnormalities including hypospadias, chordee, bilateral cryptorchidism, small scrotum, and bilateral small hydroceles were reported. No cardiac or renal abnormalities were identified. MRI of the

brain revealed global, diffuse, symmetric perisylvian polymicrogyria, mild dilatation of the lateral ventricles, colpocephaly, and cavum septum vergae (Amrom et al., 2019).

Guilherme et al. (2009) reported a duplication spanning the 2p16-p14 chromosomal region in a fetus with abnormal muscle development of the diaphragm and dysmorphic features. Amniocentesis was performed after second-trimester screening identified an increased risk of Trisomy 21. Karyotype analysis at a resolution of 550 bands identified extra genetic material on the p arm of chromosome 2, with subsequent whole chromosome painting confirming that the extra genetic material also originated from chromosome 2. Parental karyotype analysis was normal. The fetus was terminated at 23 weeks gestation, with a birth weight and length in the 50th percentile for gestational age . Reported craniofacial features included telecanthus, broad nasal root, pointed nose and chin, absent nasal bones, thin upper lip, small and low-set ears, and micrognathia. The fetus had hand abnormalities, including bilateral brachymesophalangy of the fourth fingers and dysplastic nails (Guilherme et al., 2009). Necroscopy identified small kidneys with a weight in the ~5th percentile for gestational age and an enlarged right collecting system (Guilherme et al., 2009). A histological evaluation of the kidneys identified adrenal microsteatosis (Guilherme et al., 2009). Meconium ileus was present (Guilherme et al., 2009). The diaphragm had hypoplastic musculature with an abnormally large aponeurotic central tendon (Guilherme et al., 2009). Macroscopic brain examination was normal (Guilherme et al., 2009). Microarray analysis identified a *de novo* duplication spanning the 2p16.3-p14 chromosomal bands, encompassing the following 34 genes: *GTF2A1L, LHCGR, FSHR, NRXN1, CHAC2, C2orf30, ASB3, ACYP2, C2orf73, SPTBN1, EML6, SMEK2, PNPT1, CCDC104,*

CCDC85A, VRK2, PAPOLG, BCL11A, KIAA1841, PEX13, PUS10, FANCL, REL, USP34, XPO1, COMMD1, CCT4, FAM161A, EHBP1, LOC51057, PELI1, SERTAD2, RAB1A, SPRED2 (Guilherme et al., 2009).

In a case report by Lodefalk et al. (2015), researchers describe a female patient with an interstitial duplication spanning the 2p16.1-p13.2 chromosomal region. The patient presented at two years of age with moderate to severe PTH-independent hypercalcemia, hypercalciuria, nephrocalcinosis, impaired renal function, and secondary hyperparathyroidism. Prior to the onset of symptomatic hypercalcemia, the proband had undergone previous evaluations due to general and psychomotor developmental delay, hypotonia, and a distinct pattern of dysmorphic craniofacial features. Reported craniofacial abnormalities included prominent forehead, high palate, twisted nostrils, up-slanting palpebral fissures, strabismus, and a preauricular fistula. Microarray analysis of the proband revealed a *de novo* duplication spanning the 2p16.1-p13.2 chromosomal region, with the following coordinates using the GRCh37/hg19 assembly: 55,799,737–72,298,425 (Lodefalk et al., 2015). The 16.5 Mb duplication encompasses 81 protein-coding genes.

Hypercalcemia can arise due to various environmental and genetic factors, with genetic causes encompassing both isolated and syndromic forms of the condition (Stokes et al., 2017). Common genetic mutations associated with hypercalcemia include biallelic pathogenic mutations in the calcium-sensing receptor (*CASR*) gene, which is responsible for maintaining normal serum calcium levels through regulation of parathyroid hormone production (Lodefalk et al., 2015; Stokes et al., 2017). Another autosomal recessive form of hypercalcemia is Idiopathic Infantile Hypercalcemia or IIH.

This disorder results from biallelic pathogenic mutations in either the *SLC34A1* gene (IIH1) or the *CYP24A1* gene (IIH2) (Lodefalk et al., 2015; Stokes et al., 2017). The solute carrier 34A1 (*SLC34A1*) gene encodes for a sodium-dependent phosphate transporter expressed in renal proximal tubule cells (Prié & Friedlander, 2010). This transporter regulates phosphate hemostasis through renal reabsorption of phosphate (Prié & Friedlander, 2010). Biallelic pathogenic mutations in the *SLC34A1* gene lead to reduced serum phosphate levels due to increased urinary phosphate excretion (Prié & Friedlander, 2010; Schlingmann et al., 2015). Low plasma phosphate triggers increased production of active vitamin D_3 or 1,25-dihydroxyvitamin D (1,25-$(OH)_2D_3$), which in turn stimulates increased uptake of both phosphate and calcium into the bloodstream, leading to hypercalcemia (Prié & Friedlander, 2010; Stokes et al., 2017). Biallelic pathogenic mutations in the 1,25-dihydroxyvitamin D_3 24-hydroxylase (*CYP24A1)* gene similarly result in hypercalcemia due to elevated concentrations of circulating active 1,25-$(OH)_2D_3$ (Stokes et al., 2017). The 24-hydroxylase enzyme is responsible for the degradation of active 1,25-$(OH)_2D_3$ into its biologically inactive metabolite; impaired or absent 24-hydroxylase activity results in elevated levels of 1,25-$(OH)_2D_3$, and the subsequent reabsorption of calcium into the bloodstream causes hypercalcemia (Schlingmann et al., 2015; Stokes et al., 2017). Syndromes associated with hypercalcemia include William's syndrome, Down syndrome, hypophosphatasia, and various inborn errors of metabolism (Stokes et al., 2017).

Due to the levels of calcium and intact parathyroid hormone (PTH) in the proband, treating clinicians initially suspected pathogenic mutations in the *CASR* gene; however, these suspicions were ruled out after sequencing of *CASR* failed to detect any

pathogenic alterations (Lodefalk et al., 2015). Since the patient also had abnormally elevated 1,25-$(OH)_2D_3$ at presentation, clinicians ordered sequencing of the *CYP24A1* gene to rule out IIH2, and no pathogenic variants were found. Other potential genetic causes of hypercalcemia were also ruled out, including pathogenic mutations in the *ALPL* and *NOD2* genes (Lodefalk et al., 2015). The patient's clinical presentation was also inconsistent with syndromic forms of hypercalcemia, such as Williams Syndrome, or hypercalcemia due to inborn errors of metabolism, endocrinopathies, granulomatous disorders, or malignancy (Lodefalk et al., 2015). Extensive imaging did not identify any abnormalities of the skeleton, heart, or abdomen, and ultrasounds of the parathyroid glands were normal (Lodefalk et al., 2015).

After investigating and excluding other common causes of hypercalcemia, clinicians hypothesized that the patient's hypercalcemia might be due to the dosage imbalance of genes within the 2p16.1-p13.2 duplication identified by microarray (Lodefalk et al., 2015). As discussed earlier, the concentration of circulating calcium is heavily influenced by levels of active 1,25-$(OH)_2D_3$; high plasma concentrations of active 1,25-$(OH)_2D_3$ stimulate increased calcium absorption into the bloodstream, leading to hypercalcemia (Lodefalk et al., 2015; Schlingmann et al., 2015; Stokes et al., 2017). The 1α-hydroxylase enzyme, encoded by the *CYP27B1* gene, is responsible for converting inactive vitamin D, $25(OH)D_3$ into its biologically active form, 1,25-$(OH)_2D_3$ (Schlingmann et al., 2015; Stokes et al., 2017). While the 1α-hydroxylase enzyme is well-known for generating active 1,25-$(OH)_2D_3$ in the kidney, this enzyme is also expressed in non-renal cells and tissues, including cells of the immune system (Bikle, 2020). The production of active 1,25-$(OH)_2D_3$ by 1α-hydroxylase in non-renal cells

serves paracrine and autocrine signaling purposes, rather than regulating calcium and phosphate hemostasis (Bikle, 2020; Lodefalk et al., 2015). The treating clinicians hypothesized that the 2p16.1-p13.2 duplication might cause elevated concentrations of 1,25-$(OH)_2D_3$ due to abnormal activation of the 1α-hydroxylase enzyme in non-renal cells (Lodefalk et al., 2015; Stokes et al., 2017). While the activation of *renal* 1α-hydroxylase activity is regulated by PTH, *extra-renal* activation of 1α-hydroxylase (in immune cells like macrophages) is controlled by various cytokine signaling molecules and growth factors (Bikle, 2020; Lodefalk et al., 2015). The authors propose that overexpression of *PPP3R1* (one of the genes within the proband's duplication) may increase extra-renal 1α-hydroxylase activity, leading to increased conversion of inactive $25(OH)D_3$ to active 1,25-$(OH)_2D_3$, and subsequent hypercalcemia (Lodefalk et al., 2015). The protein phosphatase three regulatory subunit B (*PPP3R1)* gene encodes for subunit B of the heterodimeric protein calcineurin (Lodefalk et al., 2015). Calcineurin is an essential immune system protein with crucial roles in the regulation of immune responses (Park et al., 2020). Calcineurin activates immune cells such as T cells, upregulates the transcription of additional immune target genes, and increases the production of cytokine signaling molecules (Lodefalk et al., 2015; Park et al., 2020). The duplicated *PPP3R1* gene was presented as a potential candidate gene for hypercalcemia, since 1α-hydroxylase is expressed in immune cells such as macrophages, and extra-renal 1α-hydroxylase activity is controlled by cytokines (Bikle, 2020; Lodefalk et al., 2015).

1.5 Purpose of Study

While the advent of chromosomal microarray testing significantly increased our ability to detect subtle copy number changes throughout the genome, it did not necessarily end the diagnostic odyssey for many patients, since some of the alterations identified had never been reported before. Our ability to detect subtle alterations and our understanding of the alteration do not always advance at the same rate. Thus, many identified changes were classified as variants of uncertain significance (VUS). As more individuals are diagnosed with rare genomic variants and data on the associated clinical characteristics are reported and shared, these VUS results can be resolved, allowing the diagnostic odyssey to end for patients and their families.

This study contains a detailed description of the clinical characteristics associated with one of these rare genetic changes with limited reports available in the literature: 2p16.1-p15 microduplications. Through the standardized collection of thorough phenotypic data for nine cases with duplications within the 2p16.1-p15 chromosomal region, this study aims to help the patients diagnosed with this rare condition and their families, by providing additional information to treating clinicians.

2. MATERIALS & METHODS

2.1 Study Overview

This study collected anonymous, de-identified genotype and phenotype information on individuals with duplications either within or including the 2p16.1-p15 chromosomal region. Data was collected from the treating clinicians (our subjects) via an anonymous, REDCap-generated survey (Harris et al., 2019; Harris et al., 2009). A letter describing the project and a survey link were sent to the treating physicians in one of two ways: through a DECIPHER administrator or through an email to clinical geneticist colleagues.

Treating clinicians recruited from DECIPHER received the study letter and survey link through a DECIPHER administrator. The data collected from the DECIPHER-administered survey is classified as non-human subjects research. The Office of Human Research Protection's (OHRP) guidance document, Engagement of Institutions in Human Subjects Research, details situations where an institution is generally considered to be either engaged or not-engaged in human subjects research. This portion of the study is considered not-engaged in human subjects research under section III.B.1 of the OHRP guidance document (See appendix A) (Office for Human Research Protections, 2021). A completed copy of the Non-Human Subject Research Determination form is maintained by the lead researcher. The data collected from the email-administered survey qualified for Self-Determination of Exempt Research under category 2i (see Appendix B) of the IRB Exempt Self-Determination Tool (University of California at Irvine Office of Research, 2021). A copy of the completed Exempt Self-

Determination Tool and any supporting documentation are maintained by the lead researcher.

2.2 Study Population, Ascertainment, & Survey Distribution

This study surveyed the treating clinicians of individuals with 2p16.1-p15 microduplications. Treating clinicians were ascertained from two cohorts: the DECIPHER database and an email list of clinical geneticist colleagues. To be included in this study, treating clinicians must follow a patient with a duplication either *within* or *including* the 2p16.1-p15 chromosomal region, confirmed by microarray analysis.

Ideal cases would only contain duplications *within* the 2p16.1-p15 chromosomal bands, since the phenotype for cases with larger duplications may be impacted by genes outside of this region. However, given the rarity of these duplication, larger duplications were not excluded. It is important to clarify that the 2p16.1-p15 Microdeletion Syndrome is caused by deletions of various sizes within a specific *portion* of the entire 2p16.1-p15 chromosomal region. Specifically, this syndrome encompasses a 2.53 Mb region of 2p16.1p15, with the following coordinates: 2:59,058,561-61,592,680 kb. Since duplications within this region are such an infrequent finding and a critical region has yet to be established, patients with duplications within the entire 2p16.1-p15 chromosomal region (2:54,700,001-63,900,000) were included in this study, rather than limiting cases to the 2.53 Mb region responsible for the deletion syndrome. Since this study aims to characterize the genetic and clinical features of individuals with 2p16.1-p15 duplications, ideal cases would not carry additional copy number variants or duplications extending beyond the 2p16.1-p15 chromosomal bands. However, cases

with larger duplications or additional copy number variants were not excluded from this study, since there may be relevant information about phenotype from the cases with larger duplications.

For the first cohort, subjects were selected from the DECIPHER database. Ascertainment of treating clinicians from DECIPHER involved identifying cases with 2p16.1-p15 duplications, evaluating each case for potential confounding factors, and selecting the cases that best fit the study inclusion criteria. First, every duplication case entered into DECIPHER that spanned the 2p16.1-p15 chromosomal region was identified, regardless of whether the duplication extended beyond the 2p16.1-p15 region of interest. Clinical information such as inheritance of the duplication, sex of the patient, phenotypic features and genomic information for each case, including the location of the duplication and the gene content, was ascertained. Some of the cases within the 2p16.1-p15 region of interest reported additional copy number variants. For cases with additional variants listed, information available in DECIPHER on the additional variant was reviewed, including the type (deletion or duplication), size (<1 Mb or >1 Mb), classification (pathogenic, likely pathogenic, variant of uncertain significance, likely benign, benign), inheritance (de novo, maternally inherited, paternally inherited, unknown), gene content, and dosage sensitivity scores for protein-coding genes. Pathogenicity classifications for variants in the DECIPHER database are entered by depositing clinicians.

A total of 46 DECIPHER cases with 2p16.1-p15 duplications were identified and the best candidates out of this list were recruited based on how well they fit the desired

study criteria. Treating clinicians received a letter describing the current project and a link to the online survey from a DECIPHER administrator.

The study team also alerted professional colleagues of the opportunity to participate in an anonymous research project if they had a patient/s with 2p16.1-p15 duplications. A letter describing the project and a link to the online survey was emailed to 350 clinical geneticist colleagues.

2.3 Survey Design

In order to further characterize the clinical manifestations associated with 2p16.1-p15 duplications, an anonymous, online survey was developed in REDCap to collect detailed genotype and phenotype information from treating clinicians (see Appendix A). The survey collected basic demographic information, such as age, chromosomal sex, and ancestry, in addition to routine genetic information such as inheritance and consanguinity. Treating physicians were also asked to specify the exact genomic coordinates of the patient's duplication as well as any additional copy number variant(s), if present. The majority of the survey focused on collecting a comprehensive history of the clinical manifestations and physical characteristics present in each patient. This portion of the survey was designed to capture any physical or developmental abnormalities across all major body systems. Questions were divided into various sections based on the location or body system affected. Within each section, commonly observed, non-specific phenotypic abnormalities were included, as well as specific features previously reported in patients with 2p16.1-p15 duplications or deletions. For each section, clinicians were asked to specify the presence or absence of each

particular characteristic as well as additional information such as laterality (for abnormalities in paired body organs) or severity (for neurodevelopmental abnormalities). Each section also included a text box where treating clinicians could enter additional information on any of the selected abnormalities within that group or add a feature that was not already included. The survey also included a text box option at the end of the entire questionnaire, which allowed treating clinicians to add any other clinically relevant information that was not specifically asked about.

The information collected through this survey was completely anonymous and de-identified. This survey did not collect any personal or identifiable information regarding the treating physician or the patient for whom they completed the survey. None of the information collected by the survey has the potential to be traced back to a specific individual.

2.4 Data Collection

Phenotypic data was collected directly from survey responses for both DECIPHER and non-DECIPHER cases. The genomic coordinates and size of the copy number variant(s) for each patient were either collected directly from survey responses (all non-DECIPHER cases and some DECIPHER cases) or downloaded from the DECIPHER database (some DECIPHER cases). Information regarding the suspected pathogenicity of each variant was either entered directly into survey responses (both non-DECIPHER and DECIPHER cases) or obtained directly from DECIPHER, when available (DECIPHER cases). For DECIPHER cases, a complete list of all of the protein-coding genes within each duplication was obtained directly from DECIPHER (all

DECIPHER cases). For non-DECIPHER cases, the genomic coordinates and reference genome build listed in the survey response were used to determine the protein-coding genes that fell within the coordinates of the duplication. A complete list of the genes within each band of chromosome 2 was obtained from the *Atlas of Genetics and Cytogenetics in Oncology and Haematology* and DECIPHER (Atlas of Genetics and Cytogenetics in Oncology and Haematology, 2021; Firth et al., 2009). For each protein-coding gene, DECIPHER also included a classification of whether the gene is likely to be dosage-sensitive, and this classification was captured in the data set. Dosage sensitivity of genes within DECIPHER variants is determined by DECIPHER. A gene is considered dose sensitive by DECIPHER if at least one dosage sensitivity predictive score (pLI, LOEUF, sHet) is in the highest category, or at least one source (GenCC, OMIM, G2P, or ClinGen) indicates that the gene is associated with disease. After collection, survey response data was stored in REDCap and secure data storage servers within the UCI health network. All genomic data comparisons were performed using GRCh37/hg19 (Kent et al., 2002).

2.5 Data Analysis

To facilitate comparisons between cases, survey responses were assigned a number from 1-10 based on the genomic coordinates of the patient's duplication, starting with the most distal 2p16.1p15 duplication and ending with the most proximal. Three tables were created to compare the characteristics of each case. The first table compared the molecular genetic features between cases and included the type of copy number variant(s) present, inheritance, expected pathogenicity (when available),

genomic coordinates, size, and gene content for each duplication. The second table, individual case summaries, captured the detailed descriptions of phenotypic features or clinical manifestations present in each case. A third table compared demographic information and the presence or absence of the various phenotypic characteristics mentioned in our survey. A figure showing comparisons of the ideograms for each of the 9 cases was generated using the UCSC genome browser and is presented in Figure 1 (Kent et al., 2002).

3. RESULTS

3.1 Overview

In total, 11 survey responses were received; eight responses were received from depositing clinicians from the DECIPHER database and three responses were received from clinical geneticists who responded to an email invitation to participate in the survey. One of the eight DECIPHER cases was excluded due to the size of the duplication within 2p (which extended well beyond the 2p16.1-p15 region of interest) and the presence of an additional large duplication spanning the q arm of chromosome 2. One of the three cases received from clinical geneticists was excluded because it represented a deletion of the 2p16.1-p15 chromosomal region, rather than a duplication. One of the DECIPHER cases carried a second duplication on the p arm of chromosome 19. This case was included in the study, however, since the duplication on chromosome 19 was classified as likely benign. In total, nine cases were included in the study. These cases were numbered from 1-9 based on the location of their breakpoints, with case 1 containing the most distal duplication start point on the p arm of chromosome 2 and case 9 containing the most proximal duplication start point.

Ideograms of the duplications listed for each of the nine cases are presented in Figure 1 according to the location of their breakpoints on chromosome 2. For cases where more than one variant is listed (cases 3 and 5), ideograms of both variants are shown in Figure 1. Case 1 contained the largest duplication, which began in the 2p16.1 chromosomal band and extended beyond our region of interest into the 2p12 chromosomal band. Case 5 contained the smallest duplication within our region of

interest, which began and ended within the 2p16.1 chromosomal band. Case 5 also carried a duplication on the p arm of chromosome 19, within the 19p12-p11 chromosomal region. In case 3, two similar duplications within the 2p16.1-p15 chromosomal region were listed. It is unclear whether the listed variants represent two *separate* duplications, or the *same* duplication detected using different testing platforms and listed twice. If the former is true, it is not possible to determine whether the duplications exist on the same or opposite chromosomes, based on the information provided. However, Figure 1 shows the variants as separate ideograms for clarity.

Figure 1: Ideograms of the 9 Duplication Cases

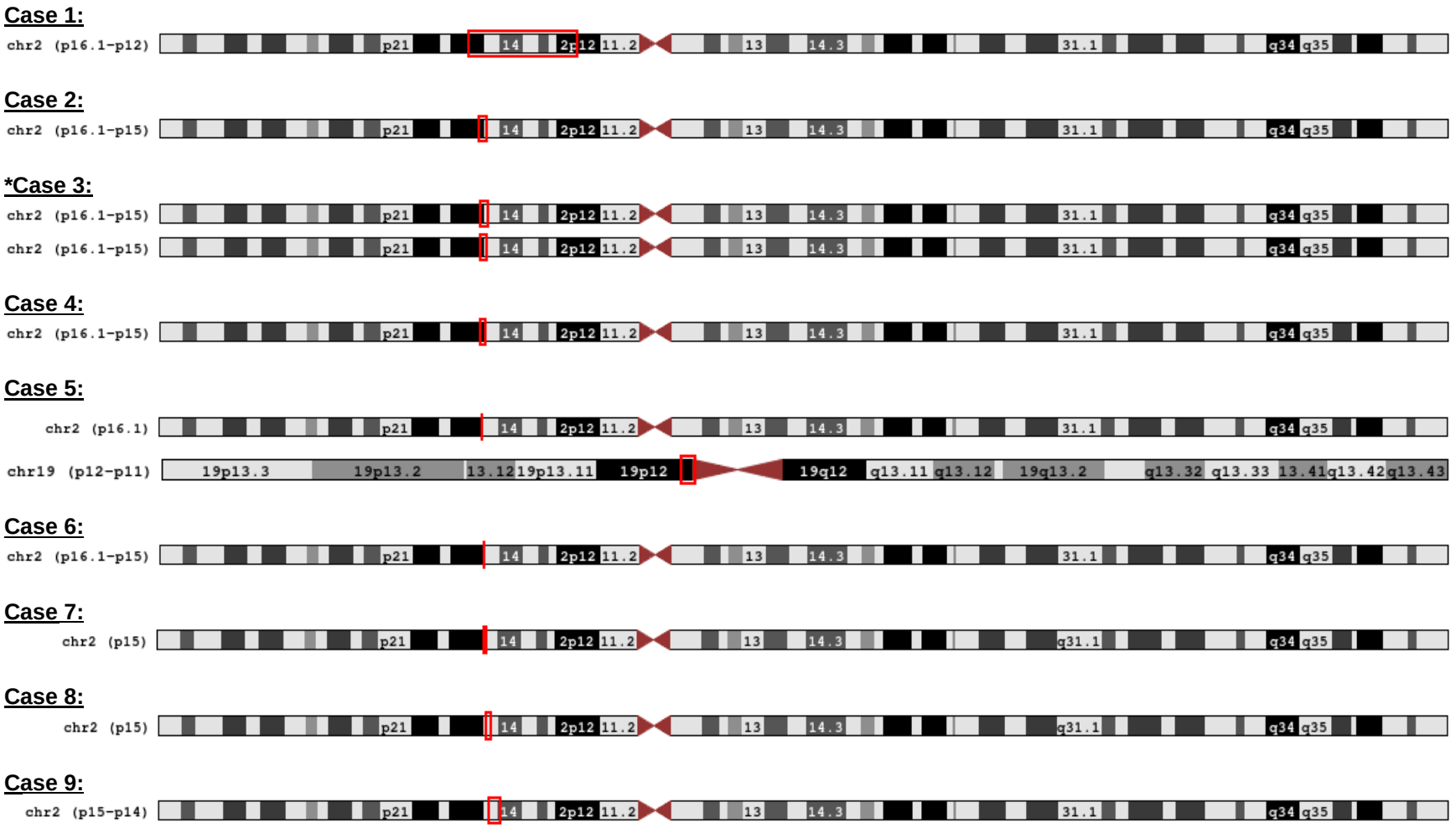

Figure 1: Ideograms of 9 cases containing duplications either *within* or *including* the 2p16.1-p15 chromosomal region. Ideograms were generated from the UCSC Genome Browser using the Human Feb. 2009 (GRCh37/hg19) Assembly (http://genome.ucsc.edu)
*Two similar duplications within the 2p16.1-p15 chromosomal region were listed for case 3. It was unclear whether these duplications reflect two separate variants or the same variant detected using different testing platforms and listed twice; if the former is true, it is impossible to determine whether the variants are in *cis* or *trans* from the information provided. Separate ideograms for each variant are shown here for clarity.

3.2 Comparison of Molecular Genetic Characteristics

The molecular genetic characteristics of nine cases with microduplications either *within* or *including* the 2p16.1-p15 chromosomal region are presented in Table 1. Table 1 displays the following for each of the nine cases: chromosomal sex, inheritance of each variant, classification of each variant (when available), coordinates of each variant, protein-coding genes within each variant and expected dose-sensitive protein coding genes for each variant.

The chromosomal sex of five out of the nine cases was 46, XX (cases 3, 4, 6, 7, 9) and the chromosomal sex of the remaining four cases was 46, XY (cases 1, 2, 5, 8), as selected in the survey response. The inheritance of the duplication was *de novo* in five cases (cases 1, 2, 3, 4, 7), inherited from an unaffected mother in two cases (cases 8 and 9), inherited from an unaffected father in one case (case 6), and unknown in one case (case 5). In two of the cases, more than one duplication was reported (case 3 and 5). Case 3 listed two duplications of different sizes (1.41 Mb and 1.17 Mb) within the same region of 2p16.1p15, both of which were classified as likely pathogenic. It is unclear whether this finding reflects the presence of two separate variants in the individual, or whether it reflects the same variant detected using different testing platforms and listed twice, thus explaining the slightly different breakpoints. Case 5 carried a 0.118 Mb duplication on chromosome 2 within the 2p16.1 chromosomal band and a 0.640 Mb duplication on chromosome 19 within the 19p12-p11 chromosomal bands; the classification of the duplication on chromosome 2 was not listed in DECIPHER but the duplication on chromosome 19 was classified as likely benign. Four of the cases (cases 2, 6, 7 and 9) carried duplications within the 2p16.1-p14

chromosomal bands ranging in size from 0.162 Mb- 2.30 Mb, all of which were classified as having uncertain pathogenicity (VUS). In two of the remaining cases (cases 1 and 4) the pathogenicity classification of the duplication was not provided. Case 1 carried a 20.5 Mb duplication within the 2p16.1-p12 chromosomal bands and case 4 carried a 0.920 Mb duplication within the 2p16.1 chromosomal band. The remaining case (case 8) carried a 1.07 Mb duplication within the 2p15 chromosomal band, classified as likely pathogenic.

The coordinates and protein coding genes for each of the duplications in the nine cases are presented in Table 1 using the UCSC Human Feb. 2009 (GRCh37/hg19) reference build. However, for case 1, the coordinates of the duplication were reported in the survey response without specifying the reference build used. The coordinates listed for case 1 may correspond to the GRCh38 reference build rather than the GRCh37/hg19 build. However, the GRCh37/hg19 and GRCh38 reference builds for these coordinates are comparable in terms of protein coding gene content. The coordinates of case 1 were entered into both assemblies to determine whether the gene content of the duplication differed between builds. The number of coding genes fully encompassed by the duplication differed by one depending on the genome build used, with the GRCH37/hg19 assembly including an additional coding gene which was not included in the duplication using the GRCh38 assembly. This region, as identified through the GRCH37/hg19 build, also includes part of another gene (*VRK2*), which is not identified as part of the region using the GRCh38 assembly.

Assuming the coordinates in case 1 were given using the GRCh37/hg19 assembly, the duplication contains 131 protein coding genes in total, starting with *VRK2*

as the most distal protein coding gene and ending with *LRRTM4* as the most proximal protein coding gene (as shown in Table 1). However, the duplication in case 1 (duplication position in GRCh37/hg19: chr2:58,254,774-78,755,462) only partially overlaps the *VRK2* gene (*VRK2* position in GRCh37/hg19: chr2:58,134,786-58,387,055). If only genes fully encompassed by the duplication were included, the duplication would contain 130 protein coding genes in total, starting with the subsequent gene, *FANCL* (*FANCL* position in GRCh37/hg19: chr2:58,386,378-58,468,515), as the most distal protein coding gene. The most proximal protein coding gene listed for case 1 would remain the same, since *LRRTM4* is fully encompassed by the duplication.

If the coordinates listed for case 1 were given using the GRCh38 genome build, the duplication would contain 129 protein coding genes in total, beginning with *BCL11A* (*BCL11A* position in GRCh38: chr2:60,450,520-60,554,467) as the most distal protein coding gene and ending with *LRRTM4* (*LRRTM4* position in GRCh38: chr2:76,747,685-77,522,376) as the most proximal protein coding gene. Both *BCL11A* and *LRRTM4* are fully encompassed by the duplication using the GRCh38 Assembly.

Table 1 lists all of the protein coding genes for each case, regardless of whether the duplication fully or partially encompasses the gene. The genes that partially disrupt a duplication are specified in the table. In case 4, the USP34 gene partially overlaps the duplication by 153.41 kb of coding region. In case 5, the *PAPOLG* gene partially overlaps the chromosome 2p16.1 duplication by 37.49 kb of coding region and the *ZNF675* gene partially overlaps the chromosome 19p12p11 duplication by 2.74 kb of coding region. In case 6, the duplication partially overlaps the *PEX13* gene by 29.12 kb of coding region. In case 7, the first and last protein coding genes (*USP34* and

COMMD1) are only partially overlapped by the duplication. The duplication overlaps the *USP34* gene by 178.96 kb of coding region and the *COMMD1* gene by 62.72 kb of coding region. In case 9, the duplication partially overlaps the *COMMD1* gene by 33.58 kb of coding region. As discussed above, the duplication in case 1 may also partially disrupt the *VRK2* gene, depending on which build truly corresponds to the coordinates provided in the survey response.

Table 1: Genetic Characteristics of 9 Cases with 2p16.1-p15 Duplications

Case	Sex	Inheritance	Classification†	Size (Mb)	Chromosomal Bands & Coordinates (GRCh37/hg19)	Protein-coding genes within duplication (distal to proximal) Suspected dose-sensitive genes are shown in bold
1	46, XY	De novo	N/A	20.5	2p16.1-p12 2:58,254,774-78,755,462*	VRK2 (partial), **FANCL**, **BCL11A**, **PAPOLG**, **REL**, PUS10, **PEX13**, KIA1841, C2orf74, **USP34**, **XPO1**, **FAM161A**, **CCT4**, COMMD1, **B3GNT2**, TMEM17, **EHBP1**, **OTX1**, **WDPCP**, **MDH1, UGP2**, **VPS54**, **PELI1**, **LGALSL**, **AFTPH**, **SERTAD2**, **SLC1A4**, CEP68, **RAB1A**, **ACTR2**, SPRED2, **MEIS1**, **ETAA1**, C1D, WDR92, PNO1, **PPP3R1**, **CNRIP1**, **PLEK**, FBXO48, APLF, PROKR1, **ARHGAP25**, **BMP10**, GKN3P, GKN2, GKN1, **ANTXR1**, **GFPT1**, **NFU1**, **AAK1**, ANXA4, GMCL1, SNRNP27, MXD1, **ASPRV1**, **PCBP1**, C2orf42, **TIA1**, PCYOX1, **SNRPG**, FAM136A, **TGFA**, **ADD2**, **FIGLA**, CLEC4F, **CD207**, **VAX2**, **ATP6V1B1**, ANKRD53, TEX261, NAGK, **MCEE**, MPHOSPH10, PAIP2B, **ZNF638**, **DYSF**, **CYP26B1**, **EXOC6B**, **SPR**, EMX1, SFXN5, RAB11FIP5, NOTO, SMYD5, PRADC1, **CCT7**, **FBXO41**, EGR4, **ALMS1**, NAT8, NAT8B, **TPRKB**, DUSP11, C2orf78, **STAMBP**, **ACTG2**, **DGUOK**, **TET3**, **BOLA3**, **MOB1A**, MTHFD2, SLC4A5, **DCTN1**, C2orf81, WDR54, RTKN, **INO80B**, INO80B-WBP1, WBP1, **MOGS**, MRPL53, CCDC142, TTC31, LBX2, **PCGF1**, TLX2, DQX1, AUP1, **HTRA2**, **LOXL3**, DOK1, **M1AP**, SEMA4F, HK2, POLE4, TACR1, EVA1A, MRPL19, GCFC2, **LRRTM4**
2	46, XY	De novo	VUS	1.47	2p16.1-p15 2:60,381,835-61,848,845	**BCL11A**, **PAPOLG**, **REL**, PUS10, **PEX13**, KIA1841, C2orf74, **USP34**, **XPO1**
3**	46, XX	De novo & De novo	Likely pathogenic & Likely pathogenic	1.41 & 1.17	2p16.1-p15 2:60,541,781-61,952,880 & 2p16.1-p15 2:60,676,037-61,848,845	**BCL11A**, **PAPOLG**, **REL**, PUS10, **PEX13**, KIA1841, C2orf74, **USP34**, **XPO1** (both)
4	46, XX	De novo	N/A	0.920	2p16.1-p15 2:60,648,296-61,568,645	**BCL11A**, **PAPOLG**, **REL**, PUS10, **PEX13**, KIA1841, C2orf74, **USP34 (partial)**

Case	Sex	Inheritance	Classification†	Size (Mb)	Chromosomal Bands & Coordinates (GRCh37/hg19)	Protein-coding genes within duplication (distal to proximal) Suspected dose-sensitive genes are shown in bold
5	46, XY	Unknown	N/A & Likely benign	0.118 & 0.640	2p16.1 2:60,986,801-61,104,424 & 19p12-p11 19:23,867,095-24,507,121	**PAPOLG (partial)** & ZNF675 (partial), ZNF681, ZNF726, ZNF254
6	46, XX	Paternally inherited (father unaffected)	VUS	0.162	2p16.1-p15 2:61,246,790-61,408,495	**PEX13 (partial)**, KIA1841, C2orf74
7	46, XX	De novo	VUS	0.677	2p15 2:61,518,864-62,195,531	**USP34 (partial)**, **XPO1**, **FAM161A**, **CCT4**, COMMD1 (partial)
8	46, XY	Maternally inherited (mother unaffected)	Likely pathogenic	1.07	2p15 2:61,804,054-62,869,158	**FAM161A**, **CCT4**, COMMD1, **B3GNT2**, TMEM17
9	46, XX	Maternally inherited (mother unaffected)	VUS	2.30	2p15-p14 2:62,329,495-64,634,038	COMMD1 (partial), **B3GNT2**, TMEM17, **EHBP1**, **OTX1**, **WDPCP**, **MDH1**, **UGP2**, **VPS54**, **PELI1**

† Pathogenicity classifications were either entered directly into survey responses or gathered from the DECIPHER database. Classifications with "N/A" correspond to cases where the pathogenicity classification was not reported in the survey response or DECIPHER.
* The coordinates of each variant are shown using GRCh37/hg19; for case 1 however, the genome build was not specified in the survey response. If using GRCH38, the duplication would begin with BCL11A as the first protein coding gene (rather than VRK2) and end with LRRTM4 as the last protein coding gene (the same as shown for GRCh37/hg19).
** Case 3 listed two overlapping duplications (as shown here); it is unclear whether this reflects the presence of two *separate* variants, or whether it reflects the *same* variant detected using different testing platforms and listed twice.
(partial) Any gene not fully encompassed by the duplication.

3.3 Individual Clinical Case Summaries

Detailed phenotypic and clinical information for each of the nine cases is presented in Table 2. Clinical case summaries were extrapolated from data entered by treating clinicians into survey responses and gathered from DECIPHER. These summaries represent aggregate data compiled from the multiple-choice options presented in the survey, DECIPHER data, as well as thorough free response answers written by the treating clinicians to provide additional information beyond what was specifically queried. The ages of the probands at entry or evaluation ranged from 1 month of age to 12 years of age.

Six cases (cases 1, 4, 5, 7, 8, 9) were noted to have either structural or signaling brain abnormalities, including polymicrogyria, increased signaling of the white matter supratentorial, asymmetric position of the chiasma and possibly delayed myelination, borderline prominence of the lateral ventricles, abnormal cerebral ventricle morphology, and mesial temporal lobe anomalies.

Cardiovascular abnormalities were described in six cases (cases 1, 2, 4, 5, 7, 8), including patent foramen ovale (PFO), fetal and neonatal idiopathic atrial flutter, atrial septal defects (ASD), ventral septal defects (VSD), patent ductus arteriosus (PDA), ventricular hypertension, abnormal ventricle morphology, and complex cardiomyopathy. In 3 cases, multiple cardiovascular abnormalities were described. Case 5 was noted to have an ASD and VSD. Case 7 was noted to have a PFO, moderate to large PDA, and right ventricular hypertension, all of which resolved by a follow-up cardiovascular appointment at 6 months of age. Case 8 was noted to have abnormal left ventricle morphology in addition to complex cardiomyopathy.

Sensorineural hearing loss was reported in two cases (cases 1 and 6). Case 1 was found to have bilateral sensorineural hearing loss and case 6 was found to have unilateral severe sensorineural hearing loss, with the following measurements: high frequency (2,000-4,000 Hz).

Head shape anomalies were described in three cases (cases 1, 4, and 5), including dolichocephaly, delayed cranial suture closure, and large head size with malar flattening. In four cases (cases 1, 2, 8, 9) abnormal head circumference measurements were reported. Case 1 reported a head circumference that was initially microcephalic but was within normal limits at a later evaluation. Case 2, 8, and 9 reported macrocephaly. The head circumference in case 2 was reported to be +2.75 DS. The head circumference in case 8 was 36.50 cm and case 9 did not report a numerical value for head circumference.

Six cases (cases 1, 2, 4, 5, 6, 7) reported abnormalities of the oral region, with 5 cases either describing an abnormality within this category that was not included in the survey checklist or providing additional information about an included abnormality. Case 1 had a philtrum with a likert scale of 1 and case 2 reported cleft of the soft palate. Case 4 reported thin upper and lower lip vermilion. Case 5 reported a smooth philtrum and thin upper lip in addition to dental abnormalities, including a conical tooth and widely spaced teeth. Case 7 reported upper and lower ankyloglossia and abnormal dentition.

Two of the nine cases (cases 8 and 9) reported a duplication inherited from an unaffected mother (see Table 1). However, the treating physician of case 9 provided additional details regarding the phenotype of the proband’s mother, presented in Table

2. In case 9, the proband's mother was reported to share similar craniofacial features as the proband but not tall stature or macrosomia.

Table 2: Individual Clinical Case Summaries of 9 Cases with 2p16.1p15 Duplications

Case	Sex	Clinical Characteristics & Case Summary
1	46, XY	The proband is a male of Hispanic/Latino ancestry; consanguinity was denied. Age at entry/evaluation was 3 years and 8 months. Genetic testing revealed a *de novo* microduplication within the 2p16.1-p12 chromosomal region, pathogenicity classification was not available. General clinical characteristics include: intrauterine growth restriction, feeding difficulty, and short stature. Neurodevelopmental abnormalities include global developmental delay. Brain abnormalities include polymicrogyria. Craniofacial features include: dolichocephaly, head circumference that was initially microcephalic but now normal, micrognathia, sparse lateral eyebrows, small ears, low-set ears, anteverted nares, philtrum likert scale 1. The proband also has unspecified vision impairment/loss and bilateral sensorineural hearing loss. Genitourinary abnormalities include hypospadias and cryptorchidism. Respiratory symptoms include wheezing and asthma. Cardiovascular abnormalities include patent foramen ovale (PFO).
2	46, XY	The proband is a male of unknown ancestry; consanguinity was denied. Age at entry/evaluation was 2 years and 11 months of age. Genetic testing revealed a *de novo* microduplication within the 2p16.1-p15 chromosomal region, classified as uncertain pathogenicity. The proband was born premature at 35 weeks + 6 days. General clinical characteristics include feeding difficulty and hypotonia. Neurodevelopmental abnormalities include global developmental delay. No brain abnormalities were identified at transfontaneller ultrasound. Craniofacial features include: macrocephaly (head circumference +2.75 SD), strabismus and cleft of the soft palate. Reported respiratory symptoms include asthma. Reported cardiovascular symptoms include fetal and neonatal idiopathic atrial flutter.
3*	46, XX	The proband is a female of Caucasian ancestry; consanguinity was denied. Age at entry/evaluation was 7 years of age. Two heterozygous *de novo* microduplications within the 2p16.1-p15 chromosomal region were listed, both of which were classified as likely pathogenic. It was unclear from the available information whether these duplications reflect two *separate* variants or the *same* variant detected using different testing platforms and listed twice. General clinical characteristics include obesity and juvenile chronic arthritis. Neurodevelopmental abnormalities include delayed speech and language development. Craniofacial features include closely spaced eyes and up-slanting palpebral fissures. Hand and feet abnormalities include small hands and feet. Genitourinary abnormalities include precocious puberty.
4	46, XX	The proband is a female of Caucasian ancestry; consanguinity was denied. Age at entry/evaluation was 12 years of age. Genetic testing revealed a *de novo* microduplication within the 2p16.1-p15 chromosomal region, pathogenicity classification was not available. General clinical characteristics include proportionate short stature. Neurodevelopmental abnormalities include global developmental delay, delayed speech and language development, and intellectual disability. Brain abnormalities include increased signaling of the white matter supratentorial. Craniofacial features include: delayed cranial suture closure, head circumference of 57 cm, frontal bossing, micrognathia, blepharophimosis, up-slanting palpebral fissures, low-set ears, wide nasal bridge, abnormality of the nasal alae, and thin upper and lower lip vermillion. Hand and feet abnormalities include tapered finger, short palm, short distal phalanges of both hands, hyperextensibility of the finger joints, and 2-3 toe syndactyly (laterality unknown). Reported cardiovascular abnormalities include atrial septal defect (ASD).
5	46, XY	The proband is a male of Caucasian ancestry; consanguinity was denied. Age at entry/evaluation was 2 years and 2 months of age. Genetic testing revealed 2 microduplications with unknown inheritance: a microduplication on chromosome 2 within the 2p16.1 chromosomal region, pathogenicity classification was not available, and a microduplication on chromosome 19 within the

Case	Sex	Clinical Characteristics & Case Summary
		19p12-p11 chromosomal region, classified as likely benign. The proband was born premature at 27 weeks + 6 days. Preeclampsia was noted. Apgar scores were 9-10-10. BW=1195g (0SD), BL= 38cm (0SD), OFC=27 cm (+1SD). Postnatal growth delay was reported with the following measurements: at 2y and 2m of age: L=82 cm (-2.7SD), W=10.3kg (-3SD), OFC=49 cm (-1SD). Weight catch-up was reported at 8 years of age with the following measurements: 22.8kg at 8 years old (-1.3SD). Lack of further information about length. General clinical characteristics include short stature and general hypotonia. Neurodevelopmental abnormalities include global developmental delay, delayed fine and gross motor development, delayed speech and language development, and intellectual disability. The proband had absent speech at 2 years and 2 months of age, but a lack of information was available about later development. The proband was noted to have general hypotonia and the following delayed motor milestones: sitting without support at 9-10 months of age and walking at 25 months of age. Brain abnormalities include asymmetric position of chiasma, without certain pathologic significance and possibly delayed myelinization. Craniofacial features include broad forehead, prominent forehead with malar flattening, relatively large head with flattened malar regions, prognathia, almond-shaped palpebral fissures, epicanthus inversus, telecanthus, low-set ears, broad nasal bridge, broad nasal tip, short nose, smooth philtrum, thin upper lip, conical tooth, and wide spaced teeth. Integumentary system abnormalities include: nevus flammeus in the glabellar, occipital, and neck region and a small (diminished) cavernous hemangioma on the right shoulder, thoracic hypertrichosis (back) and a deep sacral dimple. Reported cardiovascular abnormalities include atrial septal defect (ASD) and ventral septal defect (VSD). The patient's mother was reported to have speech delay and needed special school.
6	46, XX	The proband is a female of Caucasian ancestry; consanguinity was denied. Age at entry/evaluation was 3 years and 3 months of age. Genetic testing revealed a paternally inherited (father unaffected) microduplication within the 2p16.1-p15 chromosomal region, classified as uncertain pathogenicity. Neurodevelopmental abnormalities include global developmental delay, psychomotor retardation, delayed speech and language development, and other behavioral abnormalities including stereotypic movements. Craniofacial features include head circumference of 50.0 cm (50-75th percentile), broad nasal bridge, broad nasal tip, prominent nasal tip, long philtrum, thin upper lip, and prominent cupid's bow. Severe unilateral sensorineural hearing loss with the following measurements: right- high frequency (2,000-4,000 Hz).
7	46, XX	The proband is a female of Hispanic/Latino ancestry; consanguinity was denied. She was initially evaluated as a neonate with follow-up evaluations at 1 and 2 years of age. Genetic testing revealed a *de novo* microduplication within the 2p15 chromosomal region, classified as uncertain pathogenicity. The proband was born at 37 weeks + 1 day of age. She had a birth weight of 3.030 kg (50th percentile), birth length of 52 cm (97th percentile) and head circumference of 36 cm (97th percentile). General clinical characteristics include feeding difficulty and hypotonia. Neurodevelopmental abnormalities include mild delays in fine and gross motor development that resolved by 15 months of age. Brain abnormalities include borderline prominence of the lateral ventricles with normal architecture of the brain. Craniofacial features include prominent occiput, unilateral preauricular ear tag, upper and lower ankyloglossia, and abnormal dentition. Reported integumentary abnormalities include a lower sacrum hemangioma. Hand and feet abnormalities include bilateral postaxial polydactyly of the hands and feet, dysplastic thumbs, and bilateral cutaneous syndactyly of fingers F3-F4 and toes T2-T3. Digestive system symptoms include gastroesophageal reflux without esophagitis, diagnosed in the first months of life. Reported cardiovascular abnormalities include patent foramen ovale (PFO), a moderate to large patent ductus arteriosus (PDA), and right ventricular hypertension, all of which resolved by 6 months of age.

Case	Sex	Clinical Characteristics & Case Summary
8	46, XY	The proband is a male of Caucasian ancestry; consanguinity was denied. Age at entry/evaluation was 1 month. Genetic testing revealed a maternally inherited (mother unaffected) microduplication within the 2p15 chromosomal region, classified as likely pathogenic. Brain abnormalities include abnormal cerebral ventricle morphology. Craniofacial features include macrocephaly with a head circumference of 36.50 cm, receding/high forehead, and large ears. Digestive system abnormalities include omphalo mesenteric duct, accessory spleen. Genitourinary abnormalities include hypogonadism and cryptorchidism. Respiratory system abnormalities include a lung lobulation abnormality. Cardiovascular abnormalities include abnormal left ventricle morphology and complex cardiomyopathy. The proband was reported deceased at 3 months of age and a diagnosis of heterotaxy was suspected.
9	46, XX	The patient is a female of Caucasian ancestry; consanguinity was denied. Age at entry/evaluation was 12 years of age. Genetic testing revealed a maternally inherited (mother unaffected) microduplication within the 2p15-p14 chromosomal region, classified as uncertain pathogenicity. General clinical characteristics include tall stature. Neurodevelopmental abnormalities include delays in speech and language development. Brain abnormalities include mesial temporal lobe anomalies. Craniofacial features include macrocephaly, receding/high forehead, down-slanted palpebral fissures, and large ears. Integumentary abnormalities include a nevus on her back. Skeletal abnormalities include accelerated skeletal maturation. The proband's mother (harboring the same microduplication) was reported to show similar craniofacial conformation, but not tall stature and macrosomia.

SD= standard deviation; BW= birth weight; BL= birth length; OFC= occipitofrontal head circumference.

3.4 Comparison of Clinical Characteristics

Table 3 represents an aggregate directory of the clinical and phenotypic characteristics present in each of the nine cases. This data is displayed in checklist format, with an “x” indicating the presence of a particular feature (either reported directly in the survey response or gathered from DECIPHER). An asterisk indicates that more information is available regarding clinical characteristics within a particular category or for a particular selected feature. Below the table, information is provided for instances where the “other” option is selected. The nine cases included six cases with Caucasian ancestry (cases 3, 4, 5, 6, 8, 9), two cases with Hispanic/Latino ancestry (cases 1 and 7), and one case with unknown ancestry (case 2). Consanguinity was denied in all nine cases.

Within the general category, three cases reported feeding difficulty (cases 1, 2, and 7), three cases reported short stature (cases 1, 4, 5), and three cases reported hypotonia (cases 2, 5, 7). Global developmental delay was present in five cases (cases 1, 2, 4, 5, 6), delayed fine/gross motor development was present in three cases (case 5, 6, 7), and delayed speech/language development was present in five cases (cases 3, 4, 5, 6, 9). Two cases had intellectual disability (cases 4 and 5). Several cases shared similar craniofacial features. Cases 8 and 9 both had microcephaly, a receding/high forehead, and large ears. Eye abnormalities were present in six cases (cases 1, 2, 3, 4, 5, 9), including vision impairment/loss, sparse eyebrows, strabismus, closely spaced eyes, blepharophimosis, epicanthal folds, epicanthus inversus, and palpebral fissures. Four cases (cases 3, 4, 5, 9) reported palpebral fissure abnormalities, including up-slanting palpebral fissures (cases 3 and 4), almond shaped palpebral fissures (case 5),

and down-slanting palpebral fissures (case 9). Ear abnormalities were also common among cases, with seven cases reporting abnormalities within this category. Abnormalities within this category included hearing impairment/loss (cases 1 and 6), large ears (cases 8 and 9), small ears (case 1), low set ears (case 1, 4, 5), and an ear tag (case 7). Nasal abnormalities were a common finding, with four cases reporting abnormalities. Broad nasal bridges were reported in cases 4, 5, and 6 with cases 5 and 6 also reporting the presence of a broad nasal tip. Integumentary abnormalities were present in three cases (cases 5, 7, 9), including nevus flammeus, hemangiomas, and hypertrichosis, among others. Genitourinary abnormalities were reported in three cases (cases 1, 3, 8), including cryptorchidism, hypospadias, hypogonadism, and precocious puberty. Hand and feet abnormalities were present in three cases (cases 3, 4, 7), which included tapered fingers, finger syndactyly, toe syndactyly, and polydactyly, among others.

Table 3: Clinical Characteristics of 9 Cases with 2p16.1p15 Duplications

Case	1	2	3	4	5	6	7	8	9	N/9
Chromosomal sex:										
46, XX			x	x		x	x		x	5
46, XY	x	x			x			x		4
Inheritance:										
De Novo	x	x	x	x			x			5
Maternally inherited (mother affected)										
Maternally inherited (mother unaffected)								x	x*	2
Paternally inherited (father affected)										
Paternally inherited (father unaffected)						x				1
Unknown					x					1
Consanguinity:										
Yes										
No	x	x	x	x	x	x	x	x	x	9
Ancestry:										
Black/African American										
Hispanic/Latino	x						x			2
White			x	x	x	x		x	x	6
Asian										
American Indian/Alaska										
Native Hawaiian/Other Pacific Islander										
Unknown		x								1
General:										
IUGR	x									1
Feeding difficulty	x	x					x			3
Obesity			x							1
Short Stature	x			x	x					3
Hypertonia										
Hypotonia		x			x		x			3
Epilepsy/seizures										
Lower limb spasticity										
Recurrent infections										
Voice abnormalities										
*Other			x*		x*			x*	x*	4
Neurodevelopmental abnormalities:										
Global developmental delay	x	x		x	x*	x				5
Delayed fine/gross motor development					x*	x	x			3
Delayed speech/language development			x	x	x*	x			x	5
Intellectual disability				x	x*					2
Autism										

Case	1	2	3	4	5	6	7	8	9	N/9
Autistic traits										
ADD/ADHD										
*Other					x*	x*				2
Brain abnormalities:										
Polymicrogyria	x									1
Cortical dysplasia										
Cerebral atrophy										
Enlarged ventricles										
Hypoplasia of the corpus callosum										
Hypoplasia of the cerebellum										
Hypoplasia of the pons										
*Other				x*	x*		x*	x*	x*	5
Head shape:										
Craniosynostosis										
Brachycephaly										
Trigonocephaly										
*Other	x*				x*					2
Head circumference:										
Normal				x*	x*	x*	x*			4
Microcephaly	x*									1
Macrocephaly		x*						x*	x	3
Occiput:										
Flat										
Prominent							x			1
Forehead:										
Narrow										
Broad					x					1
Receding/high								x	x	2
Prominent					x*					1
Frontal bossing				x						1
Mandible:										
Retrognathia										
Micrognathia	x			x						2
Prognathia					x					1
Eye abnormalities:										
Optic nerve hypoplasia										
Vision impairment/loss	x									1
Palpebral fissure abnormalities			x*	x*	x*				x*	4
Blepharophimosis				x						1
Epicanthal folds										
Epicanthus inversus					x					1
Telecanthus					x					1

Case	1	2	3	4	5	6	7	8	9	N/9
Widely spaced eyes										
Closely spaced eyes			x*							1
Ptosis										
Strabismus		x								1
Fullness of eyelids (puffy)										
Sparse eyelashes										
Sparse eyebrows	x*									1
Long/straight eyelashes										
Ear abnormalities:										
Hearing impairment/loss	x*					x*				2
Large ears								x	x	2
Small ears	x									1
Low-set ears	x			x	x					3
Ear sinus										
Ear pit										
Ear tag							x*			1
Nose abnormalities:										
Anteverted nares	x									1
Broad nasal bridge				x	x	x				3
Flat nasal bridge										
Broad nasal tip					x	x				2
Prominent nasal tip						x				1
*Other				x*	x*					2
Mouth abnormalities:										
High palate										
Cleft palate		x*								1
Alveolar ridge overgrowth										
Small mouth										
Philtrum- long						x				1
Philtrum- short										
Philtrum- smooth					x					1
Down-slanted mouth corners										
Thin upper lip					x	x				2
Everted upper/lower lip vermillion										
Prominent cupid's bow						x				1
Accessory oral frenulum										
*Other	x*			x*	x*		x*			4
Integumentary system abnormalities:										
Café-au-lait spots										
Hyperpigmentation										
Nevus flammeus					x*					1

Case	1	2	3	4	5	6	7	8	9	N/9
Hemangioma					x*		x*			2
Hypertrichosis					x*					1
Hirsutism										
*Other					x*				x*	2
Digestive system abnormalities:										
Hepatomegaly										
*Other								x*		1
Genitourinary abnormalities:										
Hypogonadism								x		1
Cryptorchidism	x*							x		2
Precocious puberty			x							1
Renal cysts										
Hydronephrosis										
*Other	x*									1
Skeletal abnormalities:										
Kyphoscoliosis										
Accelerated skeletal maturation									x	1
Arthritis			x*							1
Hand and Feet abnormalities:										
Arachnodactyly										
Tapered fingers				x						1
Fifth finger clinodactyly										
3^{rd}-4^{th} finger syndactyly							x*			1
2^{nd}-3^{rd} toe syndactyly				x			x*			2
Polydactyly							x*			1
Pes planus										
*Other:			x*	x*			x*			3
Respiratory system abnormalities:										
*Other	x*	x*						x*		3
Cardiovascular system abnormalities:										
Atrial septal defect				x	x					2
Ventral septal defect					x					1
*Other	x*	x*					x*	x*		4

x= feature was reported either directly in the survey response or in the DECIPHER database.
Other, x= additional details available regarding clinical characteristics within this category or the specific feature selected. See Table 2*: Individual Clinical Case Summaries* for detailed phenotypic descriptions.
General: Juvenile arthritis (case 3), prematurity (case 5), postnatal growth delay (case 5), heterotaxy (case 8), tall stature (case 9)
Neurodevelopmental abnormalities: Absent speech (case 5), stereotypic movements (case 6)
Brain: White matter increased signaling (case 4), asymmetric chiasma (case 5), prominent lateral ventricles (case 7), abnormal ventricle morphology (case 8), mesio-temporal lobe abnormalities (case 9)
Head shape: Initial microcephaly (case 1), dolichocephaly (case 1), prominent forehead/malar flattening (case 5)

Nose abnormalities: Abnormality of the nasal alae (case 4), short nose (case 5)
Mouth abnormalities: Philtrum likert scale 1 (case 1), thin upper/lower lip vermilion (case 4), wide spaced teeth (case 5), conical tooth (case 5) upper and lower ankyloglossia (case 7), abnormal dentition (case 7)
Integumentary system abnormalities: Deep sacral dimple (case 5), nevus (case 9)
Digestive system abnormalities: Omphalo mesenteric duct, accessory spleen (case 8)
Genitourinary abnormalities: Hypospadias (case 1)
Hand and feet abnormalities: Small extremities (case 3), short palms, bilateral short distal phalanges of the hands, hypextensible fingers (case 4), dysplastic thumbs (case 7)
Respiratory system abnormalities: Asthma (case 1, 2), lobulation anomaly (case 8)
Cardiovascular system abnormalities: Patent foramen ovale (case 1,7), atrial flutter (case 2), patent ductus arteriosus (case 7), right ventricular hypertension (case 7), abnormal left ventricle morphology (case 8), complex cardiomyopathy (case 8)

4. DISCUSSION

4.1 Literature Comparisons & Genotype-Phenotype analysis

The most commonly reported clinical manifestations in this study include neurodevelopmental abnormalities, structural or signaling brain abnormalities, cardiac anomalies, and various dysmorphic facial features. These findings are consistent with previous published cases of duplications within the 2p16.1-p15 chromosomal region, which also identified neurodevelopmental delays, brain and cardiac abnormalities, and a similar pattern of dysmorphic facial features. Similar to literature cases of 2p16.1-p15 microduplications, no reports of autistic traits or autism were reported, which appears to be a key clinical difference between duplications and deletions of this region. Interestingly, behavioral concerns were also not reported in any of the 9 cases included in this study, which differs from other published cases of 2p16.1-p15 microduplications. Additionally, no cases in this study reported attention deficit hyperactivity disorder (ADD/ADHD), obsessive compulsive disorder (OCD), or behavioral concerns such as temper tantrums, aggression, or oppositional behavior, which are included in several published reports of microduplications including the 2p16.1-p15 chromosomal region. Two cases containing more proximal duplications reported sensorineural hearing loss, which has recently been linked to duplications within the 2p14 chromosomal region (Lezirovitz et al., 2020). However, only one of the cases in this study extended into the 2p14 region.

Cardiovascular abnormalities were reported in 67% of the cases in this study. Cardiac abnormalities included patent foramen ovale (PFO), fetal and neonatal

idiopathic flutter, atrial septal defect (ASD), ventral septal defect (VSD), patent ductus arteriosus (PDA), right ventricular hypertension, abnormal left ventricle morphology and complex cardiomyopathy. In three of the cases, multiple cardiovascular abnormalities were described. Case 5 was noted to have an ASD and VSD. Case 7 was noted to have a PFO, moderate to large PDA, and right ventricular hypertension and case 8 was noted to have abnormal left ventricle morphology in addition to complex cardiomyopathy. This finding is significant because while cardiac abnormalities are reported in published cases, they are only reported in two of the five published 2p16.1-p15 microduplication cases (or 22%) and one of the cases describing larger duplications extending beyond the 2p16.1-p15 chromosomal region.

Upon review of the limited number of patients with duplications either within or including the 2p16.1-p15 chromosomal region, cardiac abnormalities were reported in a total of three previously published cases (two cases specifically describing 2p16.1-p15 microduplications, and one case describing a much larger interstitial duplication of 2p). A mild patent arterial duct with left to right shunting was reported in the 12 year old male proband described by Pavone et al. (2019). He carried a duplication within the 2p16.1-p15 chromosomal bands, encompassing *BCL11A*, *PAPOLG*, *REL*, *PUS10*, *PEX13*, *KIAA1841*, *C2orf74*, *ASHA*, *USP34*, and *XPO1* (Pavone et al., 2019). Cardiac abnormalities were also reported in the second patient described by Lovrecic et al. (2018). The 5 year old male proband had two hemodynamically significant atrial septal defects and mild dilation of the right ventricle (Lovrecic et al., 2018). He carried a duplication within the 2p16.1p15 chromosomal region encompassing the following genes: *BCL11A, PAPOLG, REL, PUS10, PEX13, USP34, XPO1, FAM161A, CCT4,*

COMMD1, and *B3GNT2.* Mild pulmonary artery stenosis was reported in the first patient described by Amron et al. (2019), who carried a larger duplication spanning the 2p16.3-p13.3 chromosomal region.

In this study, case 5 carried smallest duplication of all the patients identified with cardiac abnormalities. He carried a duplication fully encompassed within the 2p16.1 chromosomal band, with partial disruption of only one protein coding gene, *PAPOLG*. The *PAPOLG* gene is also duplicated in case 4, 2, and 1 of this study, along with all three of the literature cases. The duplicated genes in case 7 and case 8 overlap with the larger duplication in case 1 and the larger duplication reported in the literature by Amron et al., (2019). However, case 7 and case 8 do not include the *PAPOLG* gene that is disrupted in case 5 of this study and duplicated in all of the other duplication cases associated with cardiac abnormalities (case 1, 2, 4 in this study and all three literature cases). Case 7 also has partial overlap with the duplicated *USP34* gene in case 4 and the *USP34* and *XPO1* genes in case 2.

This study also identified common dysmorphic craniofacial features among cases that show some consistent overlap with published reports for patients with 2p16.1-p15 microduplications. Macrocephaly was present in 33% of the 9 cases in this study, and a common feature in multiple reports of 2p16.1-p15 microduplications. Three of the nine cases (case 4, 5, and 6) in this study reported broad nasal bridge, which is also reported in one of the 2p16.1-p15 microduplication literature cases and three of the larger literature cases of duplications extending beyond the 2p16.1-p15 region of interest. Low-set ears were also reported in three of the nine cases in this study (1, 3, and 4) and three of the literature cases describing duplications extending beyond

2p16.1-p15. Interestingly, palpebral fissure abnormalities were reported in four of the nine cases (case 3, 4, 5, and 9) but only one of the literature cases describing larger microduplications extending beyond 2p16.1-p15. There appears to be common dysmorphic craniofacial features between patients in this study, however variability was also identified based on the location of the duplication. Two of the cases in this study (case 8 and 9), reported very similar craniofacial features, with both cases reporting a macrocephaly, receding/high forehead, and large ears. These cases also carried similar duplications at the more proximal boundary of the 2p16.1-p15 region of interest, with overlap of the following duplicated protein coding genes: *COMMD1, B3GNT2,* and *TMEM17.* Two cases reported micrognathia (cases 1 and 4) which was only reported in one of the literature cases describing larger duplications.

While this study identified common craniofacial features between cases, there was only partial overlap with literature case reports. However, this can be partially explained by the small sample size of literature cases for this condition. There does appear to be commonality among cases in this study, with some variability based on the location of the duplication. Notably, a very similar pattern of craniofacial abnormalities was reported in two of the cases with the most proximal duplications. As more individuals are reported with 2p16.1-p15 microduplications, the association of duplications with a specific pattern of craniofacial features may become more clear.

Genitourinary abnormalities were reported in two of the cases in this study (case 1 and 8) that contained more proximal duplications; case 1 carried a duplication encompassing the 2p16.1-p12 chromosomal region and case 8 carried a duplication within the 2p15 chromosomal bands. Cryptorchidism and hypospadias were reported in

case 1 and cryptorchidism and hypogonadism in case 8. Upon review of the literature, genitourinary abnormalities were only present in two of the microduplication cases that extended well beyond the 2p16.1-p15 chromosomal region, both of which were reported by Amrom et al. (2019). Both patients carried larger duplications extending beyond the 2p16.1-p15 chromosomal region, similar to case 1. The first patient described by Amrom et al. (2019) carried a 2p16.3-p13.3 duplication and the third patient carried a 2p24.1-p13.1 duplication. Case 1 and the two literature cases overlap by many genes. Case 8, encompassing a small duplication within 2p15, only contains the following protein coding genes: *FAM161A, CCT4, COMMD1, B3GNT2,* and *TMEM17.* These genes are also encompassed by the duplications in the two literature cases and case 1, however more research is needed to before a link between these genes and genitourinary defects can be confirmed or excluded.

Interestingly, there appears to be some phenotypic overlap between the features of the 9 cases described here and published cases of individuals with 2p16.1-p15 Microdeletion Syndrome. Genitourinary abnormalities were reported in two of the nine cases in this report carrying duplications that encompassed more proximal locations within the region of interest. Genitourinary abnormalities are also reported in individuals with microdeletions of this region, and the 2p15 chromosomal band was proposed as a potential critical region associated with this finding by Jorgez et al. (2014). However, case 8 in this study does not contain the *OTX1* gene within the duplication. Other common findings for both deletions and duplications of this region include developmental delay, intellectual disability, and structural and signaling brain abnormalities; however, the structural brain abnormalities identified in the deletions are

different to those currently reported in the literature for the duplications. While these similarities may be due to the heterogenous nature of the abnormalities or the limited number of reports for 2p16.1-p15 microduplications, it is also possible that disruption of specific gene(s) within this region, whether due to haploinsufficiency or triplosensitivity, leads to disorganization of similar developmental pathways resulting in a common phenotypic outcome.

4.2 Limitations & Benefits of Study

These findings add valuable information to the limited body of knowledge regarding the clinical manifestations associated with duplications within the 2p16.1-p15 chromosomal region. Duplications of this region are extremely rare, with only five case reports currently available in the literature that describe this condition, and three case reports describing duplications extending beyond the 2p16.1-p15 chromosomal region of interest. In this study, cardiac abnormalities were among the most commonly reported findings. Cardiac abnormalities were also identified in three of the literature cases with duplications of this region; the cases described by Pavone et al. (2019) and Lovrecic et al. (2018) carried duplications within the 2p16.1p15 chromosomal bands, while the case by Amron et al. (2019) carried a larger deletion encompassing the 2p16.3-p13.3 chromosomal bands. This is in contrast to individuals with 2p16.1-p15 Microdeletion Syndrome, who do not typically carry cardiac defects.

Limitations of the study include comparisons between individuals evaluated at different ages and between individuals carrying duplications of various sizes and gene content. Despite these limitations, this study also had several benefits. One of the main

strengths of this study is the standardized method of data collection. The survey collected detailed phenotypic information on each patient in a very structured way across all body systems. Standardized collection of data is important to draw meaningful comparisons between individuals, however this method of collection is not always possible, especially for such a rare condition. The same survey instrument was used to collect detailed information across all of the potentially relevant domains from each treating physician. By including features of previously published cases for both the duplication and deletion syndrome, the survey also allows researchers to better determine whether specific features of interest are truly not present in the individual or just not reported. This mode of data collection will facilitate future comparisons of features as more affected individuals are identified.

4.3 Summary & Significance

The identification of *any* copy number changes within the 2p16.1-p15 chromosomal bands is extremely rare; however, microduplications within the 2p16.1-p15 chromosomal region are an especially infrequent finding, with only five reports currently available in the literature. While reported individuals with 2p16.1-p15 microduplications share similar clinical characteristics, including dysmorphic facial features, congenital anomalies, and developmental delay, the heterogeneous nature of the abnormalities and small sample size make it difficult to determine whether microduplications of this region constitute a reciprocal (yet milder) syndrome to 2p16.1-p15 Microdeletion Syndrome.

This study thoroughly describes the clinical and molecular genetic characteristics of nine additional patients harboring 2p16.1-p15 microduplications. Comparisons of these nine patients with reports in the literature confirm a consistent pattern of neurodevelopmental abnormalities and dysmorphic features in patients with 2p16.1-p15 microduplications. While additional reports are necessary to further delineate the characteristics associated with this condition and the critical region(s) responsible for specific features, these findings provide valuable information that has the potential to improve medical management and patient care.

The most common clinical manifestations identified in the nine cases in this study included neurodevelopmental abnormalities (present in 89%) including global developmental delays and delayed speech and language development (56%), delayed fine and gross motor development (33%), structural or signaling brain abnormalities (67%) and cardiac anomalies (67%). Interestingly, there were no cases of autism or attention deficits in these 9 cases. The presence of these anomalies in the majority of affected individuals has important implications on potential screening and surveillance recommendations, despite the small sample size. Treating clinicians seeing a patient diagnosed with 2p16.1-p15 microduplication may consider further imaging studies such as an echocardiogram or brain MRI, in addition to early intervention programs (with physical, occupational, or speech therapies), if appropriate.

REFERENCES

1. Amrom, D., Poduri, A., Goldman, J. S., Dan, B., Deconinck, N., Pichon, B., Nadaf, J., Andermann, F., Andermann, E., Walsh, C. A., & Dobyns, W. B. (2019). Duplication 2p16 is associated with perisylvian polymicrogyria. *American Journal of Medical Genetics Part A*, *179*(12), 2343–2356. https://doi.org/10.1002/ajmg.a.61342

2. Ansorge, R. (2011, January 9). *FISH Test*. WebMD. Retrieved November 5, 2021, from https://www.webmd.com/cancer/fish-cancer-test

3. Atlas of Genetics and Cytogenetics in Oncology and Haematology. (2021). *List by chromosome of all genes in Atlas: Chromosome 2*. Retrieved November 16, 2021, from http://atlasgeneticsoncology.org/Indexbychrom/idxg_2.html

4. Bagheri, H., Badduke, C., Qiao, Y., Colnaghi, R., Abramowicz, I., Alcantara, D., Dunham, C., Wen, J., Wildin, R. S., Nowaczyk, M. J., Eichmeyer, J., Lehman, A., Maranda, B., Martell, S., Shan, X., Lewis, S. M., O'Driscoll, M., Gregory-Evans, C. Y., & Rajcan-Separovic, E. (2016). Identifying candidate genes for 2p15p16.1 microdeletion syndrome using clinical, genomic, and functional analysis. *JCI Insight*, *1*(3). https://doi.org/10.1172/jci.insight.85461

5. Bejjani, B. A., & Shaffer, L. G. (2006). Application of Array-Based Comparative Genomic Hybridization to Clinical Diagnostics. *The Journal of Molecular Diagnostics*, *8*(5), 528–533. https://doi.org/10.2353/jmoldx.2006.060029

6. Bikle, D. D. (2020). Vitamin D: Newer Concepts of Its Metabolism and Function at the Basic and Clinical Level. *Journal of the Endocrine Society*, *4*(2). https://doi.org/10.1210/jendso/bvz038

7. Bishop, R. (2010). Applications of fluorescence in situ hybridization (FISH) in detecting genetic aberrations of medical significance. *Bioscience Horizons*, *3*(1), 85–95. https://doi.org/10.1093/biohorizons/hzq009

8. Case, S. (2020, July 27). *History and Evolution of Cytogenetics*. Behind the Bench. Retrieved October 6, 2021, from https://www.thermofisher.com/blog/behindthebench/history-and-evolution-of-cytogenetics/

9. Chen, C. P., Chern, S. R., Wu, P. S., Chen, S. W., Lai, S. T., Chuang, T. Y., Chen, W. L., Yang, C. W., & Wang, W. (2018). Prenatal diagnosis of a 3.2-Mb 2p16.1-p15 duplication associated with familial intellectual disability. *Taiwanese Journal of Obstetrics and Gynecology*, *57*(4), 578–582. https://doi.org/10.1016/j.tjog.2018.06.018

10. Chen, C. P., Chern, S. R., Wu, P. S., Chen, S. W., Wu, F. T., & Wang, W. (2021). Prenatal diagnosis of familial 2p15 microduplication associated with pulmonary artery stenosis, single umbilical artery and left foot postaxial polydactyly on fetal

ultrasound. *Taiwanese Journal of Obstetrics and Gynecology*, *60*(1), 161–164. https://doi.org/10.1016/j.tjog.2020.11.025

11. Chial, H. (2008). *Cytogenetic Approaches for Studying Human Disease: Flow Cytometry, CGH, and FISH*. Nature Education. Retrieved October 13, 2021, from https://www.nature.com/scitable/topicpage/cytogenetic-methods-and-disease-flow-cytometry-cgh-772/

12. Cui, C., Shu, W., & Li, P. (2016). Fluorescence In situ Hybridization: Cell-Based Genetic Diagnostic and Research Applications. *Frontiers in Cell and Developmental Biology*, *4*. https://doi.org/10.3389/fcell.2016.00089

13. di Gregorio, E., Savin, E., Biamino, E., Belligni, E. F., Naretto, V. G., D′Alessandro, G., Gai, G., Fiocchi, F., Calcia, A., Mancini, C., Giorgio, E., Cavalieri, S., Talarico, F., Pappi, P., Gandione, M., Grosso, M., Asnaghi, V., Restagno, G., Mandrile, G., . . . Brusco, A. (2014). Large cryptic genomic rearrangements with apparently normal karyotypes detected by array-CGH. *Molecular Cytogenetics*, *7*(1), 82. https://doi.org/10.1186/s13039-014-0082-7

14. Drets, M. E., & Shaw, M. W. (1971). Specific Banding Patterns of Human Chromosomes. *Proceedings of the National Academy of Sciences*, *68*(9), 2073–2077. https://doi.org/10.1073/pnas.68.9.2073

15. Durmaz, A. A., Karaca, E., Demkow, U., Toruner, G., Schoumans, J., & Cogulu, O. (2015). Evolution of Genetic Techniques: Past, Present, and Beyond. *BioMed Research International*, *2015*, 1–7. https://doi.org/10.1155/2015/461524

16. Edwards, J., Harnden, D., Cameron, A., Crosse, V., & Wolf, O. (1960). A NEW TRISOMIC SYNDROME. *The Lancet*, *275*(7128), 787–790. https://doi.org/10.1016/s0140-6736(60)90675-9

17. Fannemel, M., Barøy, T., Holmgren, A., Rødningen, O. K., Haugsand, T. M., Hansen, B., Frengen, E., & Misceo, D. (2014). Haploinsufficiency of XPO1 and USP34 by a de novo 230 kb deletion in 2p15, in a patient with mild intellectual disability and cranio-facial dysmorphisms. *European Journal of Medical Genetics*, *57*(9), 513–519. https://doi.org/10.1016/j.ejmg.2014.05.008

18. Félix, T. M., Petrin, A. L., Sanseverino, M. T. V., & Murray, J. C. (2010). Further characterization of microdeletion syndrome involving 2p15-p16.1. *American Journal of Medical Genetics Part A*, *152A*(10), 2604–2608. https://doi.org/10.1002/ajmg.a.33612

19. Ferguson-Smith, M. A. (2015). History and evolution of cytogenetics. *Molecular Cytogenetics*, *8*(1). https://doi.org/10.1186/s13039-015-0125-8

20. Firth, H. V., Richards, S. M., Bevan, A. P., Clayton, S., Corpas, M., Rajan, D., Vooren, S. V., Moreau, Y., Pettett, R. M., & Carter, N. P. (2009). DECIPHER: Database of Chromosomal Imbalance and Phenotype in Humans Using Ensembl Resources. *The American Journal of Human Genetics*, *84*(4), 524–533. https://doi.org/10.1016/j.ajhg.2009.03.010

21. Guilherme, R., Guimiot, F., Tabet, A. C., Khung-Savatovsky, S., Gauthier, E., Nouchy, M., Benzacken, B., Verloes, A., Oury, J. F., Delezoide, A. L., & Aboura, A. (2009). Abnormal muscle development of the diaphragm in a fetus with 2p14-p16 duplication. *American Journal of Medical Genetics Part A*, *149A*(12), 2892–2897. https://doi.org/10.1002/ajmg.a.33135

22. Hammer, R. D., Doll, D., Layfield, L., Reichard, K. K., Hanson, C. A., Kurtin, P. J., Howard, M. T., Litzow, M. R., van Dyke, D. L., Ketterling, R. P., Wiktor, A. E., & He, R. (2016). Correspondence: Is It Time for a New Gold Standard? FISH vs Cytogenetics in AML Diagnosis. *American Journal of Clinical Pathology*, *145*(3), 430–432. https://doi.org/10.1093/ajcp/aqw008

23. Hand, J. L. (2021, July). *Recessive X-linked ichthyosis*. UpToDate. https://www.uptodate.com/contents/recessive-x-linked-ichthyosis

24. Hanna, T. P., King, W. D., Thibodeau, S., Jalink, M., Paulin, G. A., Harvey-Jones, E., O'Sullivan, D. E., Booth, C. M., Sullivan, R., & Aggarwal, A. (2020). Mortality due to cancer treatment delay: systematic review and meta-analysis. *BMJ (Clinical Research Ed.)*, m4087. https://doi.org/10.1136/bmj.m4087

25. Harewood, L., & Fraser, P. (2014). The impact of chromosomal rearrangements on regulation of gene expression. *Human Molecular Genetics*, *23*(R1), R76–R82. https://doi.org/10.1093/hmg/ddu278

26. Harris, P. A., Taylor, R., Minor, B. L., Elliott, V., Fernandez, M., O'Neal, L., McLeod, L., Delacqua, G., Delacqua, F., Kirby, J., & Duda, S. N. (2019). The REDCap consortium: Building an international community of software platform partners. *Journal of Biomedical Informatics*, 95, 103208. https://doi.org/10.1016/j.jbi.2019.103208

27. Harris, P. A., Taylor, R., Thielke, R., Payne, J., Gonzalez, N., & Conde, J. G. (2009). Research electronic data capture (REDCap)—A metadata-driven methodology and workflow process for providing translational research informatics support. Journal of Biomedical Informatics, 42(2), 377–381. https://doi.org/10.1016/j.jbi.2008.08.010

28. Henrichsen, C. N., Chaignat, E., & Reymond, A. (2009). Copy number variants, diseases and gene expression. Human Molecular Genetics, 18(R1), R1–R8. https://doi.org/10.1093/hmg/ddp011

29. Houck, M. (2012). Chapter 13 - Classical Cytogenetics: Karyotyping. In S. E. Peterson & J. F. Loring (Eds.), *Human Stem Cell Manual: A Laboratory Guide* (2nd ed., pp. 187–202). Academic Press.

30. Jang, W., Kim, Y., Han, E., Park, J., Chae, H., Kwon, A., Choi, H., Kim, J., Son, J. O., Lee, S. J., Hong, B. Y., Jang, D. H., Han, J. Y., Lee, J. H., Kim, S. Y., Lee, I. G., Sung, I. K., Moon, Y., Kim, M., & Park, J. H. (2019). Chromosomal Microarray Analysis as a First-Tier Clinical Diagnostic Test in Patients With Developmental Delay/Intellectual Disability, Autism Spectrum Disorders, and Multiple Congenital

Anomalies: A Prospective Multicenter Study in Korea. *Annals of Laboratory Medicine*, *39*(3), 299–310. https://doi.org/10.3343/alm.2019.39.3.299

31. Jobanputra, V., Esteves, C., Sobrino, A., Brown, S., Kline, J., & Warburton, D. (2011). Using FISH to increase the yield and accuracy of karyotypes from spontaneous abortion specimens. *Prenatal Diagnosis*, *31*(8), 755–759. https://doi.org/10.1002/pd.2759

32. Jorde, L. B., Carey, J. C., & Bamshad, M. J. (2015). Clinical Cytogenetics: The Chromosomal Basis of Human Disease. In *Medical Genetics* (5th ed., pp. 103–108). Elsevier.

33. Jorgez, C. J., Rosenfeld, J. A., Wilken, N. R., Vangapandu, H. V., Sahin, A., Pham, D., Carvalho, C. M. B., Bandholz, A., Miller, A., Weaver, D. D., Burton, B., Babu, D., Bamforth, J. S., Wilks, T., Flynn, D. P., Roeder, E., Patel, A., Cheung, S. W., Lupski, J. R., & Lamb, D. J. (2014). Genitourinary Defects Associated with Genomic Deletions in 2p15 Encompassing OTX1. *PLoS ONE*, *9*(9), e107028. https://doi.org/10.1371/journal.pone.0107028

34. Kannan, T. P., & Zilfalil, B. A. (2009). Cytogenetics: Past, Present and Future. *The Malaysian Journal of Medical Sciences*, *16*(2), 4–9.

35. Kent, W. J., Sugnet, C. W., Furey, T. S., Roskin, K. M., Pringle, T. H., Zahler, A. M., & Haussler, A. D. (2002). The Human Genome Browser at UCSC. *Genome Research*, *12*(6), 996–1006. https://doi.org/10.1101/gr.229102

36. Kniffin, C. L. (2016, February 15). *#612513 Chromosome 2p16.1-p15 deletion syndrome*. Online Mendelian Inheritance in Man (OMIM). Retrieved December 2021, from https://omim.org/entry/612513#geneMap

37. Kulkarni, S., PhD, Cottrell, C. E., PhD, & Al-Kateb, H., MSc, PhD. (2012). Cytogenetics. In P. A. Humphrey MD, L. P. Dehner MD, & J. D. Pfeifer MD (Eds.), *The Washington Manual of Surgical Pathology* (2nd ed., pp. 863–873). Lippincott Williams & Wilkins.

38. Ledbetter, D. H. (2008). Cytogenetic Technology — Genotype and Phenotype. *New England Journal of Medicine*, *359*(16), 1728–1730. https://doi.org/10.1056/nejme0806570

39. Lejeune, J., Turpin, R., & Gautier, M. (1959). Chromosomic diagnosis of mongolism. *Archives Francaises de Pediatrie*, *16*, 962–963.

40. Levy, B., & Burnside, R. D. (2019). Are all chromosome microarrays the same? What clinicians need to know. *Prenatal Diagnosis*, *39*(3), 157–164. https://doi.org/10.1002/pd.5422

41. Lezirovitz, K., Vieira-Silva, G. A., Batissoco, A. C., Levy, D., Kitajima, J. P., Trouillet, A., Ouyang, E., Zebarjadi, N., Sampaio-Silva, J., Pedroso-Campos, V., Nascimento, L. R., Sonoda, C. Y., Borges, V. M., Vasconcelos, L. G., Beck, R. M. O., Grasel, S. S., Jagger, D. J., Grillet, N., Bento, R. F., . . . Oiticica, J. (2020). A rare genomic duplication in 2p14 underlies autosomal dominant hearing loss

DFNA58. *Human Molecular Genetics*, *29*(9), 1520–1536. https://doi.org/10.1093/hmg/ddaa075

42. Li, M. M., & Andersson, H. C. (2009). Clinical Application of Microarray-Based Molecular Cytogenetics: An Emerging New Era of Genomic Medicine. *The Journal of Pediatrics*, *155*(3), 311–317. https://doi.org/10.1016/j.jpeds.2009.04.001

43. Lodefalk, M., Frykholm, C., Esbjörner, E., & Ljunggren, S. (2015). Hypercalcaemia in a Patient with 2p13.2-p16.1 Duplication. *Hormone Research in Paediatrics*, *85*(3), 213–218. https://doi.org/10.1159/000442747

44. Lovrecic, L., Gnan, C., Baldan, F., Franzoni, A., Bertok, S., Damante, G., Isidor, B., & Peterlin, B. (2018). Microduplication in the 2p16.1p15 chromosomal region linked to developmental delay and intellectual disability. *Molecular Cytogenetics*, *11*(39). https://doi.org/10.1186/s13039-018-0388-y

45. Mefford, H. C. (2009). Genotype to phenotype—discovery and characterization of novel genomic disorders in a “genotype-first” era. *Genetics in Medicine*, *11*(12), 836–842. https://doi.org/10.1097/gim.0b013e3181c175d2

46. Merck Manuals, & Powell-Hamilton, N. (2020, June). *Microdeletion and Microduplication Syndromes*. Merck Manuals Professional Edition. Retrieved September 29, 2021, from https://www.merckmanuals.com/professional/pediatrics/chromosome-and-gene-anomalies/microdeletion-and-microduplication-syndromes#

47. Miller, D. T. (2021, August 22). *Prenatal diagnosis of chromosomal imbalance: Chromosomal microarray*. UpToDate. Retrieved November 27, 2021, from https://www.uptodate.com/contents/prenatal-diagnosis-of-chromosomal-imbalance-chromosomal-microarray

48. Miller, D. T., Adam, M. P., Aradhya, S., Biesecker, L. G., Brothman, A. R., Carter, N. P., Church, D. M., Crolla, J. A., Eichler, E. E., Epstein, C. J., Faucett, W. A., Feuk, L., Friedman, J. M., Hamosh, A., Jackson, L., Kaminsky, E. B., Kok, K., Krantz, I. D., Kuhn, R. M., . . . Ledbetter, D. H. (2010). Consensus Statement: Chromosomal Microarray Is a First-Tier Clinical Diagnostic Test for Individuals with Developmental Disabilities or Congenital Anomalies. *The American Journal of Human Genetics*, *86*(5), 749–764. https://doi.org/10.1016/j.ajhg.2010.04.006

49. Mimouni-Bloch, A., Yeshaya, J., Kahana, S., Maya, I., & Basel-Vanagaite, L. (2015). A de-novo interstitial microduplication involving 2p16.1-p15 and mirroring 2p16.1-p15 microdeletion syndrome: Clinical and molecular analysis. *European Journal of Paediatric Neurology*, *19*(6), 711–715. https://doi.org/10.1016/j.ejpn.2015.07.013

50. Nguyen, T., MD, PhD, Hassan, A., MD, & Perry, A., MD. (2012). Fluorescence in situ hybridization. In P. A. Humphrey MD, L. P. Dehner MD, & J. D. Pfeifer MD (Eds.), *The Washington Manual of Surgical Pathology* (2nd ed., pp. 876–886). Lippincott Williams & Wilkins.

51. Nussbaum, R. L., McInnes, R. R., & Willard, H. F. (2015). *Thompson & Thompson Genetics in Medicine* (8th ed.). Elsevier.

52. O'Connor, C. (2008a). *Fluorescence In Situ Hybridization (FISH)*. Nature Education. Retrieved October 13, 2021, from https://www.nature.com/scitable/topicpage/fluorescence-in-situ-hybridization-fish-327/

53. O'Connor, C. (2008b). *Karyotyping for Chromosomal Abnormalities*. Nature Education. Retrieved October 9, 2021, from https://www.nature.com/scitable/topicpage/karyotyping-for-chromosomal-abnormalities-298/

54. Office for Human Research Protections (OHRP). (2021, September 21). *Engagement of Institutions in Human Subjects Research (2008)*. U.S. Department of Health & Human Services. Retrieved November 12, 2021, from https://www.hhs.gov/ohrp/regulations-and-policy/guidance/guidance-on-engagement-of-institutions/index.html

55. Parmar, A., & Chan, K. K. W. (2020). Prioritising research into cancer treatment delays. *BMJ*, 371-m4261. https://doi.org/10.1136/bmj.m4261

56. Pavone, P., Falsaperla, R., Rizzo, R., Praticò, A. D., & Ruggieri, M. (2019). Chromosome 2p15-p16.1 microduplication in a boy with congenital anomalies: Is it a distinctive syndrome? *European Journal of Medical Genetics*, *62*(1), 47–54. https://doi.org/10.1016/j.ejmg.2018.05.001

57. Rajcan-Separovic, E., Harvard, C., Liu, X., McGillivray, B., Hall, J. G., Qiao, Y., Hurlburt, J., Hildebrand, J., Mickelson, E. C. R., Holden, J. J. A., & Lewis, M. E. S. (2007). Clinical and molecular cytogenetic characterisation of a newly recognised microdeletion syndrome involving 2p15-16.1. *Journal of Medical Genetics*, *44*(4), 269–276. https://doi.org/10.1136/jmg.2006.045013

58. Shaffer, L. G., & Bejjani, B. A. (2004). A cytogeneticist's perspective on genomic microarrays. *Human Reproduction Update*, *10*(3), 221–226. https://doi.org/10.1093/humupd/dmh022

59. Shaffer, L. G., Theisen, A., Bejjani, B. A., Ballif, B. C., Aylsworth, A. S., Lim, C., McDonald, M., Ellison, J. W., Kostiner, D., Saitta, S., & Shaikh, T. (2007). The discovery of microdeletion syndromes in the post-genomic era: review of the methodology and characterization of a new 1q41q42 microdeletion syndrome. *Genetics in Medicine*, *9*, 607–616. https://doi.org/10.1097/gim.0b013e3181484b49

61. Shimojima, K., Okamoto, N., & Yamamoto, T. (2015). Characteristics of 2p15-p16.1 microdeletion syndrome: Review and description of two additional patients. *Congenital Anomalies*, *55*(3), 125–132. https://doi.org/10.1111/cga.12112

62. Sinclair, A. (2002). Genetics 101: cytogenetics and FISH. *CMAJ : Canadian Medical Association Journal*, *167*(4), 373–374.

63. Smetana, J., Fröhlich, J., Vranová, V., Mikulášová, A., Kuglík, P., & Hájek, R. (2011). Oligonucleotide-based array CGH as a diagnostic tool in multiple myeloma patients. *Klin Onkol*, *24(Suppl):*, S43–S48.

64. Smith, D. W., Patau, K., Therman, E., & Inhorn, S. L. (1960). A new autosomal trisomy syndrome: multiple congenital anomalies caused by an extra chromosome. *The Journal of Pediatrics*, *57*(3), 338–345. https://doi.org/10.1016/s0022-3476(60)80241-7

65. Spinner, N. B. (2013). Chromosome Banding. In S. Maloy, & K. Hughes (Eds.), *Brenner's Encyclopedia of Genetics* (2nd ed., pp. 546–548). Academic Press.

66. Theisen, A., PhD. (2008). *Microarray-based Comparative Genomic Hybridization (aCGH)*. Nature Education. https://www.nature.com/scitable/topicpage/microarray-based-comparative-genomic-hybridization-acgh-45432

67. Traylor, R. N., Bruno, D. L., Burgess, T., Wildin, R., Spencer, A., Ganesamoorthy, D., Amor, D. J., Hunter, M., Caplan, M., Rosenfeld, J. A., Theisen, A., Torchia, B. S., Shaffer, L. G., Ballif, B. C., & Slater, H. R. (2010). A Genotype-First Approach for the Molecular and Clinical Characterization of Uncommon De Novo Microdeletion of 20q13.33. *PLoS ONE*, *5*(8), e12462. https://doi.org/10.1371/journal.pone.0012462

68. Uhrig, S., Schuffenhauer, S., Fauth, C., Wirtz, A., Daumer-Haas, C., Apacik, C., Cohen, M., Müller-Navia, J., Cremer, T., Murken, J., & Speicher, M. R. (1999). Multiplex-FISH for Pre- and Postnatal Diagnostic Applications. *The American Journal of Human Genetics*, *65*(2), 448–462. https://doi.org/10.1086/302508

69. University of California at Irvine Office of Research. (2021). *Exempt Self Determination Tool*. UCI Office of Research. Retrieved December 11, 2021, from https://www.research.uci.edu/compliance/human-research-protections/researchers/Exempt-Self-Determination-Tool.html

70. UT Health San Antonio. (2020, September 4). *FISH – PRODUCTS OF CONCEPTION*. UT Health Science Center San Antonio Department of Pathology and Laboratory Medicine. Retrieved November 3, 2021, from https://lsom.uthscsa.edu/pathology/reference-labs/clinical-molecular-cytogenetics/fish-products-of-conception/

71. Watson, C. T., Tomas, M. B., Sharp, A. J., & Mefford, H. C. (2014). The Genetics of Microdeletion and Microduplication Syndromes: An Update. *Annual Review of Genomics and Human Genetics*, *15*(1), 215–244. https://doi.org/10.1146/annurev-genom-091212-153408

72. Wohlleber, E., Kirchhoff, M., Zink, A. M., Kreiß-Nachtsheim, M., Küchler, A., Jepsen, B., Kjaergaard, S., & Engels, H. (2011). Clinical and molecular characterization of two patients with overlapping de novo microdeletions in 2p14-p15 and mild mental retardation. *European Journal of Medical Genetics*, *54*(1), 67–72. https://doi.org/10.1016/j.ejmg.2010.09.012

73. Wolff, D. J. (2013). Chapter 17: Fluorescence In Situ Hybridization (FISH). In S. L. Gersen & M. B. Keagle (Eds.), *The Principles of Clinical Cytogenetics* (3rd ed., pp. 415–436). Springer.

APPENDIX A:

Engagement of Institutions in Human Subjects Research III.B.1

III. Interpretation of Engagement of Institutions in Human Subjects Research:

B. Institutions Not Engaged in Human Subjects Research: Institutions would be considered not engaged in an HHS-conducted or supported non-exempt human subjects research project (and, therefore, would not need to hold an OHRP-approved FWA or certify IRB review and approval to HHS) if the involvement of their employees or agents in that project is limited to one or more of the following. The following are scenarios describing the types of institutional involvement that would make an institution not engaged in human subjects research;

1. Institutions whose employees or agents perform commercial or other services for investigators provided that all of the following conditions also are met:

    a. the services performed do not merit professional recognition or publication privileges

    b. the services performed are typically performed by those institutions for non-research purposes

    c. the institution's employees or agents do not administer any study intervention being tested or evaluated under the protocol

APPENDIX B:

Self-Determination of Exempt Research 2i)

Self-Determination of Exempt Research is allowable in the following categories if the criteria in 2i) or 2ii) are met.

Category 2: Research that includes only interactions involving educational tests (cognitive, diagnostic, aptitude, achievement), survey procedures, interview procedures, or observation of public behavior (including visual or auditory recording).

2i) The information obtained is recorded by the investigator in such a manner that the identity the human subjects CANNOT readily be ascertained, either directly or through identifiers linked to the subjects.

APPENDIX C:

Blank Template of Survey Instrument

Clinical and Molecular Characterization of 2p16.1-p15 Microduplications: a genotype-phenotype analysis

The same link can be used to complete the survey for multiple patients. Thank you very much in advance for participating in this survey. There is limited data available in the literature on this microduplication, so your responses are extremely valuable.

For questions that require a single answer, please select the best choice. For questions that allow multiple answers, please select all that apply. Additional details can be added when the 'other' option is selected.

Decipher ID: _____

Type of copy number variant:

- ◯ Microduplication
- ◯ Microdeletion
- ◯ Other

You selected "other" for copy number variant. Please specify in the text box: _____

Base pair coordinates of microduplication or microdeletion:
(please also include coordinates of other copy number variants if present)

Age at entry/evaluation: _____

Chromosomal sex:

- ◯ 46 XX
- ◯ 46 XY
- ◯ Other

You selected "other" for chromosomal sex. Please specify in the text box: _____

Inheritance:

- ◯ De Novo
- ◯ Maternally inherited (mother affected)
- ◯ Maternally inherited (mother unaffected)
- ◯ Paternally inherited (father affected)
- ◯ Paternally inherited (father unaffected)
- ◯ Unknown

Consanguinity:

- ◯ Yes
- ◯ No
- ◯ Unknown

You selected "yes" for consanguinity. Please specify degree of relationship if known: _____

Ancestry:

- ◯ Black/African American
- ◯ Hispanic/Latino
- ◯ White
- ◯ Asian
- ◯ American Indian/Alaska Native
- ◯ Native Hawaiian/Other Pacific Islander
- ◯ Unknown
- ◯ Other

You selected "other" for ancestry. Please specify in the text box: _____

General (please select all that apply):

- ☐ None
- ☐ IUGR (intrauterine growth restriction)
- ☐ Feeding difficulty
- ☐ Obesity
- ☐ Short Stature
- ☐ Hypertonia
- ☐ Hypotonia
- ☐ Hypogonadism
- ☐ Epilepsy/seizures
- ☐ Lower limb spasticity
- ☐ Recurrent infections
- ☐ Voice abnormalities (hoarse/nasal)
- ☐ Other

You selected "other" for general. Please specify in the text box: _____

Neurodevelopmental abnormalities (please select all that apply):

- ☐ None
- ☐ Global developmental delay
- ☐ Delayed fine/gross motor development
- ☐ Delayed speech/language development
- ☐ Intellectual disability
- ☐ Autism
- ☐ Autistic traits
- ☐ ADD/ADHD
- ☐ Other

You selected "intellectual disability" for neurodevelopmental abnormalities. Please specify severity if known:

- ◯ Mild
- ◯ Moderate
- ◯ Severe

You selected "other" for neurodevelopmental abnormalities. Please specify in the text box: _____

Brain abnormalities (please select all that apply):
Based on brain MRI or CT scan.

- ☐ None
- ☐ Polymicrogyria
- ☐ Cortical dysplasia
- ☐ Cerebral atrophy
- ☐ Enlarged ventricles
- ☐ Hypoplasia of the corpus callosum
- ☐ Hypoplasia of the cerebellum
- ☐ Hypoplasia of the pons
- ☐ Other

You selected "other" for brain abnormalities. Please specify in the text box:	_____
Head shape:	◯ No abnormality ◯ Craniosynostosis ◯ Brachycephaly ◯ Trigonocephaly ◯ Other
You selected "other" for head shape. Please specify in the text box:	_____
Head circumference:	◯ Normal ◯ Microcephaly ◯ Macrocephaly ◯ Unknown
Please specify head circumference in cm if known:	_____
Occiput:	◯ Normal ◯ Flat ◯ Prominent ◯ Other
You selected "other" for occiput. Please specify in the text box:	_____
Forehead (please select all that apply):	☐ Normal ☐ Narrow ☐ Broad ☐ Receding/high ☐ Prominent ☐ Frontal bossing ☐ Other
You selected "other" for forehead. Please specify in the text box:	_____
Mandible:	◯ Normal ◯ Retrognathia ◯ Micrognathia ◯ Prognathia ◯ Other
You selected "other" for mandible. Please specify in the text box:	_____

Eye abnormalities (please select all that apply):	☐ None ☐ Optic nerve hypoplasia ☐ Vision impairment/loss ☐ Palpebral fissure abnormalities ☐ Blepharophimosis ☐ Epicanthal folds ☐ Epicanthus inversus ☐ Telecanthus ☐ Widely spaced eyes ☐ Closely spaced eyes ☐ Ptosis ☐ Strabismus ☐ Fullness of eyelids (puffy) ☐ Sparse eyelashes ☐ Sparse eyebrows ☐ Long/straight eyelashes ☐ Other
You selected "palpebral fissure abnormalities" for eye abnormalities. Please specify type if known:	◯ Up-slanted Palpebral fissures ◯ Down-slanted Palpebral fissures ◯ Almond-shaped Palpebral fissures ◯ Long Palpebral fissures ◯ Short Palpebral fissures
You selected "other" for eye abnormalities. Please specify in the text box:	_____
Ear abnormalities (please select all that apply):	☐ None ☐ Hearing impairment/loss ☐ Large ears ☐ Small ears ☐ Low-set ears ☐ Ear sinus ☐ Ear pit ☐ Ear tag ☐ Other
You selected "hearing impairment/loss" for ear abnormalities. Please specify laterality if known:	◯ Unilateral ◯ Bilateral ◯ Unknown
You selected "ear sinus" for ear abnormalities. Please specify laterality if known:	◯ Unilateral ◯ Bilateral ◯ Unknown
You selected "ear pit" for ear abnormalities. Please specify laterality if known:	◯ Unilateral ◯ Bilateral ◯ Unknown
You selected "ear tag" for ear abnormalities. Please specify laterality if known:	◯ Unilateral ◯ Bilateral ◯ Unknown
You selected "other" for ear abnormalities. Please specify in the text box:	_____

Nose abnormalities (please select all that apply):	☐ None ☐ Anteverted nares ☐ Broad nasal bridge ☐ Flat nasal bridge ☐ Broad nasal tip ☐ Prominent nasal tip ☐ Other
You selected "other" for nose abnormalities. Please specify in the text box:	_____
Mouth abnormalities (please select all that apply):	☐ None ☐ High palate ☐ Cleft palate ☐ Alveolar ridge overgrowth ☐ Small mouth ☐ Philtrum- long ☐ Philtrum- short ☐ Philtrum- Smooth ☐ Down-slanted mouth corners ☐ Thin upper up ☐ Everted upper/lower lip vermillion ☐ Prominent cupid's bow ☐ Accessory oral frenulum ☐ Other
You selected "other" for mouth abnormalities. Please specify in the text box:	_____
Integumentary system abnormalities (please select all that apply):	☐ None ☐ Café-au-lait spots ☐ Hyperpigmentation ☐ Nevus flammeus ☐ Hemangioma ☐ Hypertrichosis ☐ Hirsutism ☐ Other
You selected one or more abnormalities for integumentary system. Please specify location/details in the text box:	_____
You selected "other" for integumentary system abnormalities. Please specify in the text box:	_____
Digestive system abnormalities (please select all that apply):	☐ None ☐ Hepatomegaly ☐ Other
You selected "other" for digestive system abnormalities. Please specify in the text box:	_____
Lymphatic system abnormalities (please select all that apply):	☐ None ☐ Splenomegaly ☐ Other
You selected "other" for lymphatic system abnormalities. Please specify in the text box:	_____

Hematological abnormalities (please select all that apply):	☐ None ☐ Anemia ☐ Thrombocytopenia ☐ Neutropenia ☐ Persistent fetal hemoglobin ☐ Other
You selected "other" for hematological abnormalities. Please specify in the text box:	_____
Genitourinary abnormalities (please select all that apply):	☐ None ☐ Hypogonadism ☐ Cryptorchidism ☐ Precocious puberty ☐ Renal cysts ☐ Hydronephrosis ☐ Other
You selected "other" for genitourinary abnormalities. Please specify in the text box:	_____
Skeletal abnormalities (please select all that apply):	☐ None ☐ Kyphoscoliosis ☐ Accelerated skeletal maturation ☐ Arthritis ☐ Other
You selected "other" for skeletal abnormalities. Please specify in the text box:	_____
Hand and Feet abnormalities (please select all that apply):	☐ None ☐ Arachnodactyly ☐ Tapered fingers ☐ Fifth finger clinodactyly ☐ 2nd-3rd finger syndactyly ☐ 2nd-3rd toe syndactyly ☐ Polydactyly ☐ Pes planus ☐ Other
You selected "fifth finger clinodactyly" for hand and feet abnormalities. Please specify laterality if known:	◯ Unilateral ◯ Bilateral ◯ Unknown
You selected "2nd-3rd finger syndactyly" for hand and feet abnormalities. Please specify laterality if known:	◯ Unilateral ◯ Bilateral ◯ Unknown
You selected "2nd-3rd toe syndactyly" for hand and feet abnormalities. Please specify laterality if known:	◯ Unilateral ◯ Bilateral ◯ Unknown
You selected "polydactyly" for hand and feet abnormalities. Please specify laterality if known:	◯ Unilateral ◯ Bilateral ◯ Unknown
You selected "polydactyly" for hand and feet abnormalities. Please specify details in the text box:	_____

You selected "other" for hand and feet abnormalities. Please specify details in the text box:	_____
Respiratory system abnormalities:	◯ None ◯ Other
You selected "other" for respiratory system abnormalities. Please specify in the text box:	_____
Endocrine system abnormalities:	◯ None ◯ Other
You selected "other" for endocrine system abnormalities. Please specify in the text box:	_____
Cardiovascular system abnormalities (please select all that apply):	☐ None ☐ Atrial septal defect ☐ ventral septal defect ☐ Other
You selected "other" for cardiovascular system abnormalities. Please specify in the text box:	_____

Please add any additional phenotype data that may be relevant in the text box below: